the plant journal

SEB SOCIETY FOR EXPERIMENTAL BIOLOGY

The Plant Journal (2020) **101,** 858–873 doi: 10.1111/tpj.14587

SI ADVANCES IN PHOTOSYNTHESIS

Mesophyll conductance in land surface models: effects on photosynthesis and transpiration

Jürgen Knauer[1,2,*], Sönke Zaehle[2,3], Martin G. De Kauwe[4], Vanessa Haverd[1], Markus Reichstein[2,3] and Ying Sun[5]

[1]*CSIRO Oceans and Atmosphere, Canberra, ACT 2601, Australia,*

[2]*Department of Biogeochemical Integration, Max Planck Institute for Biogeochemistry, 07745 Jena, Germany,*

[3]*Michael-Stifel Center Jena for Data-Driven and Simulation Science, 07745 Jena, Germany,*

[4]*ARC Centre of Excellence for Climate Extremes and the Climate Change Research Centre, University of New South Wales, Sydney, 2052 NSW, Australia, and*

[5]*School of Integrative Plant Science, Soil and Crop Sciences Section, Cornell University, Ithaca, NY 14850, USA*

Received 5 July 2019; revised 10 October 2019; accepted 17 October 2019; published online 28 October 2019.
*For correspondence (e-mail juergen.knauer@csiro.au).

SUMMARY

The CO_2 transfer conductance within plant leaves (mesophyll conductance, g_m) is currently not considered explicitly in most land surface models (LSMs), but instead treated implicitly as an intrinsic property of the photosynthetic machinery. Here, we review approaches to overcome this model deficiency by explicitly accounting for g_m, which comprises the re-adjustment of photosynthetic parameters and a model describing the variation of g_m in dependence of environmental conditions. An explicit representation of g_m causes changes in the response of photosynthesis to environmental factors, foremost leaf temperature, and ambient CO_2 concentration, which are most pronounced when g_m is small. These changes in leaf-level photosynthesis translate into a stronger climate and CO_2 response of gross primary productivity (GPP) and transpiration at the global scale. The results from two independent studies show consistent latitudinal patterns of these effects with biggest differences in GPP in the boreal zone (up to ~15%). Transpiration and evapotranspiration show spatially similar, but attenuated, changes compared with GPP. These changes are indirect effects of g_m caused by the assumed strong coupling between stomatal conductance and photosynthesis in current LSMs. Key uncertainties in these simulations are the variation of g_m with light and the robustness of its temperature response across plant types and growth conditions. Future research activities focusing on the response of g_m to environmental factors and its relation to other plant traits have the potential to improve the representation of photosynthesis in LSMs and to better understand its present and future role in the Earth system.

Keywords: leaf internal CO_2 transfer, plant gas exchange, photosynthesis, transpiration, Earth system modelling.

INTRODUCTION

Photosynthesis requires CO_2 to diffuse from the free atmosphere through the leaf boundary layer, the stomata, and the leaf internal structures to the chloroplasts inside plant leaf cells. Mesophyll conductance to CO_2 transfer (g_m) describes the last part of this diffusional pathway: the ease with which CO_2 from the intercellular airspaces diffuses to the stroma of the chloroplasts in the mesophyll cells where carboxylation occurs. g_m is defined by Fick's first law:

$$g_m = A_n/(C_i - C_c) \quad (1)$$

where A_n is the rate of net photosynthesis, C_i is the intercellular CO_2 concentration, and C_c is the chloroplastic CO_2 concentration. Equation (1) suggests that g_m is a central component of the gas exchange system of plants, as it affects – together with the two other main conductances in the CO_2 pathway, stomatal conductance (g_s), and leaf boundary layer conductance – the CO_2 concentration available for photosynthesis. This aspect makes g_m seem relevant for consideration in land surface models (LSMs), which upscale calculations of photosynthesis at the leaf

scale to produce canopy, regional, and global estimates of photosynthesis (Bonan *et al.*, 2011; Rogers *et al.*, 2017). Photosynthesis – at canopy and larger scales commonly represented as gross primary productivity (GPP) – is the primary flux of carbon into terrestrial ecosystems and strongly influences ecosystem carbon storage. As the carbon and water cycles are closely linked, understanding photosynthesis is also important for the world's water cycle and associated feedbacks with the land surface energy balance and global climate (Bonan, 2008). Simulations of GPP in LSMs depend on a multitude of factors and feedbacks, but the simulated large-scale carbon uptake by vegetation is primarily determined by how it is represented at the leaf level. In fact, LSM simulations of continental water, carbon, and energy fluxes have been repeatedly shown to be sensitive to alterations of physiological processes at the leaf level (Sellers *et al.*, 1996; Friend and Kiang, 2005; Gedney *et al.*, 2006; Booth *et al.*, 2012; Smith *et al.*, 2016; Knauer *et al.*, 2017; Lemordant *et al.*, 2018). Therefore, any model components affecting simulations of photosynthesis at the leaf level require detailed consideration in the development and application of LSMs.

In most state-of-the-art LSMs, g_m is considered only implicitly as part of the photosynthetic machinery, and g_s represents the only biological diffusion barrier for CO_2. One reason for this lack of representation is that g_m is dependent on many factors, not all of which are well understood. The inverse value of g_m, the mesophyll resistance ($r_m = 1/g_m$) can be expressed as the sum of several resistances in series in both the gaseous and liquid phase within the leaf: the intercellular airspaces, the cell wall, the plasma membrane, the cytosol, the chloroplast envelope, and the chloroplast stroma (Evans *et al.*, 2009; Terashima *et al.*, 2011). These individual resistances are, to different extents, controlled by both leaf anatomical and biochemical determinants (Flexas *et al.*, 2018). The thickness of the cell wall and the chloroplast area attached to the intercellular airspaces (S_c) have been identified as important anatomical predictors of g_m (Evans *et al.*, 1994; Tomás *et al.*, 2013). The most relevant biochemical factors include the (temperature-dependent) solubility and diffusivity of CO_2 in the liquid phase (von Caemmerer and Evans, 2015), the catalytic activity of carbonic anhydrase (CA), which alleviates the diffusion of CO_2 in the chloroplast stroma, as well as the presence of aquaporins that transport CO_2 ('cooporins') (Terashima *et al.*, 2006), which facilitate CO_2 transfer across cell membranes (Perez-Martin *et al.*, 2014). g_m plays a role in all photosynthetic pathways (C3, C4, and CAM), but g_m in C4 plants does not include the chloroplast envelope and stroma components (von Caemmerer, 2000), which means that C_c in Equation (1) has to be replaced by the CO_2 concentration in the cytosol of the mesophyll cells (C_m) in C4 plants.

The fact that g_m is affected by both leaf anatomy and biochemistry has two important implications for modelling leaf internal CO_2 transfer at the large scale. First, g_m varies significantly across plant types, with more robust leaves as, for example, found in evergreen needle-leaf trees showing lower maximum g_m values than those with a softer structure as for example found in most herbs. Variations in g_m caused by leaf anatomy can also be found between sun and shade leaves within the same plants (Warren *et al.*, 2007). Second, g_m is not static, but changes not only throughout the lifetime of a leaf (Niinemets *et al.*, 2006; Barbour *et al.*, 2016), but also rapidly (at the timescale of minutes) in response to environmental cues such as leaf temperature or CO_2 concentration (Flexas *et al.*, 2012). In the following, we review how g_m is currently considered and implemented in LSMs, and what effects g_m has on large-scale simulations of photosynthesis and transpiration. In the last section, we identify key uncertainties in the simulation of g_m at larger scales and discuss strategies for future model development.

IMPLEMENTATION OF MESOPHYLL CONDUCTANCE INTO LSMS

Most photosynthesis models in LSMs are based on the model of Farquhar *et al.* (1980), which simulates A_n as the minimum of three rates: carboxylation-limited photosynthesis (A_c), RuBP regeneration-limited photosynthesis (A_j), and photosynthesis limited by triose phosphate utilization (TPU) (A_p):

$$A_n = \min(A_c, A_j, A_p) - R_l \quad (2)$$

$$A_c = \frac{V_{cmax}(C_i - \Gamma^*)}{C_i + K_c(1 + O_i/K_o)} \quad (3)$$

$$A_j = \frac{J/4(C_i - \Gamma^*)}{C_i + 2\Gamma^*} \quad (4)$$

$$A_p = 3\text{TPU} \quad (5)$$

where R_l is mitochondrial respiration in the light, V_{cmax} is the maximum carboxylation rate, Γ^* is the chloroplastic CO_2 compensation point, K_c and K_o are the Michaelis-Menten constants for CO_2 and O_2, respectively, O_i is the intercellular O_2 concentration, and J is the rate of electron transport. In many cases, TPU limitation is not considered as a third (sink-limited) limitation state in Equation (2). As TPU limitation is relevant only at high C_i when the effects of g_m are lowest, the effects of TPU limitation are presumably minor and will not be discussed in full detail throughout this review.

As can be seen in Equations (3) and (4), the Farquhar *et al.* (1980) model makes the assumption that the available CO_2 concentration for photosynthesis is C_i, which corresponds to an infinite g_m. This assumption originates historically, as early estimates of g_m (e.g. Hall, 1971) were too high (>2 mol m^{-2} sec^{-1}) to significantly affect the available CO_2 concentration (von Caemmerer, 2000). Yet, the application of measurement techniques that emerged in the

following years (Evans *et al.*, 1986; Harley *et al.*, 1992) has repeatedly confirmed that g_m is low enough to cause a significant drawdown from C_i to C_c, as well as to limit photosynthesis to a similar extent as stomatal conductance (g_s).

The presence of such a, now widely recognized, significant difference between C_i and C_c raises the question of why g_m is still ignored in many recent applications of the Farquhar *et al.* (1980) model in general and most state-of-the-art LSMs in particular. The reason for this neglect is primarily that parameters in the Farquhar *et al.* (1980) model are determined by observations (in this case mostly A_n-C_i curves, see Changes to A_n-C_i curves), that already contain information about g_m. In this sense, the Farquhar *et al.* (1980) model accounts for g_m in an implicit manner by using parameters that are determined on a C_i-basis. The use of these C_i-based (or 'apparent') parameters (instead of C_c-based or 'true' parameters) compensate to a great extent for the overestimation of available CO_2 for photosynthesis and allow the use of C_i (instead of C_c) in Equations (3) and (4), with sufficient accuracy in many cases.

An alternative to this g_m-implicit formulation of the Farquhar *et al.* (1980) model (Equations 2–5) as used by most LSMs is to simulate g_m explicitly. In this case, g_m is determined by a separate model and used to calculate C_c according to Equation (1). C_c can then be used instead of C_i in the same formulations as in the implicit case, hence structural modifications must not necessarily be made to the model. However, since parameters in the implicit model are determined on a C_i-basis, photosynthetic parameters must also be re-estimated on a C_c basis (i.e. adjusted from their 'apparent' to 'true' values) if g_m is modelled explicitly. This adjustment does not only affect the two parameters describing photosynthetic capacity (V_{cmax} and J_{max}), but also the RuBisCO kinetic constants (K_c, K_o, Γ^*), all of which represent values valid at C_i only (Bernacchi *et al.*, 2002; Ethier and Livingston, 2004; Warren, 2008b). Importantly, including an additional conductance term into a photosynthesis model without adjusting other parameters would lead to a double-accounting of g_m (implicitly and explicitly), which would result in the underestimation of the magnitude of photosynthesis and the overestimation of its CO_2 sensitivity.

In the following, the two key aspects of implementing an explicit representation of g_m into photosynthesis models for use in LSMs are described: first, the g_m model itself, and, second, approaches to adjust photosynthetic parameters in the encompassing photosynthesis model.

Mesophyll conductance models in LSMs

General form. Several models have been described that simulate g_m at cell (Tholen and Zhu, 2011) and leaf level (Niinemets and Reichstein, 2003; Tomás *et al.*, 2013; Xiao and Zhu, 2017). These models resolve the contribution of individual subconductances in the gaseous and liquid phases as well as the role of different sinks and sources of CO_2 from different cell components (Tholen *et al.*, 2012; Gu and Sun, 2014; Yin and Struik, 2017) based on anatomical and in some cases also biochemical factors. To date, models with this degree of detail were not implemented in LSMs. This is mainly because of insufficient data to extrapolate these formulations to larger scales. For example, in the absence of measurements of the conductances of individual cell components across plant types, the parameterization of individual conductances would very likely lead to problems of equifinality, which compromises the tractability of the model and its predictive power with respect to changing environmental conditions. A more tractable approach for use in LSMs is to combine all the individual conductances to form one total g_m and not explicitly resolve biochemical processes. Simpler models like this relate g_m linearly to g_s (Ohsumi *et al.*, 2007; Cai *et al.*, 2008; Vico and Porporato, 2008), to leaf N (Ohsumi *et al.*, 2007), directly to A_n (Yin *et al.*, 2009), or to A_n and leaf water potential (Dewar *et al.*, 2017). However, to the knowledge of the authors, none of these have been applied at large spatial scales.

In LSMs, g_m has so far been implemented as empirical, multiplicative formulations, which can be written in a generalized form as (Suits *et al.*, 2005; Sun *et al.*, 2014a; Knauer *et al.*, 2019):

$$g_m = g_{m,max25} \cdot f_L(L) \cdot f_T(T_l) \cdot f_W(\theta) \quad (6)$$

where $g_{m,max25}$ is the unstressed g_m at 25°C and at the top of the canopy, f_L describes the variation of g_m across the canopy profile in dependence of the leaf area index (L), and f_T and f_W are leaf temperature (T_l) and soil moisture (θ) response functions, respectively. $g_{m,max25}$ is treated as a PFT-specific model parameter that accounts for differences in maximum g_m values across plant types. $g_{m,max25}$ has been parameterized from a relationship with other photosynthetic leaf traits such as V_{cmax} (Suits *et al.*, 2005), from a relationship with other structural plant traits (Sun *et al.*, 2014a), or directly from leaf-level measurements (Knauer *et al.*, 2019; Figure 1).

It is physiologically meaningful to include a minimum g_m value into Equation (6) (e.g. as a minimum function; Knauer *et al.*, 2019) as it is unlikely that g_m will reach values of 0, which would imply a leaf interior that is completely impermeable to CO_2 transfer. The existence of a non-zero minimum g_m has been supported by measurements in which g_m did not decrease to 0 even under extreme conditions of water stress (Galmés *et al.*, 2007; Perez-Martin *et al.*, 2009; Limousin *et al.*, 2010).

Response to environmental factors. The functions in Equation (6) represent responses of g_m to environmental factors on instantaneous (minutes) to intermediate (days to months) time scales that were often reported throughout the literature [Figure 2; see Flexas *et al.* (2012) and

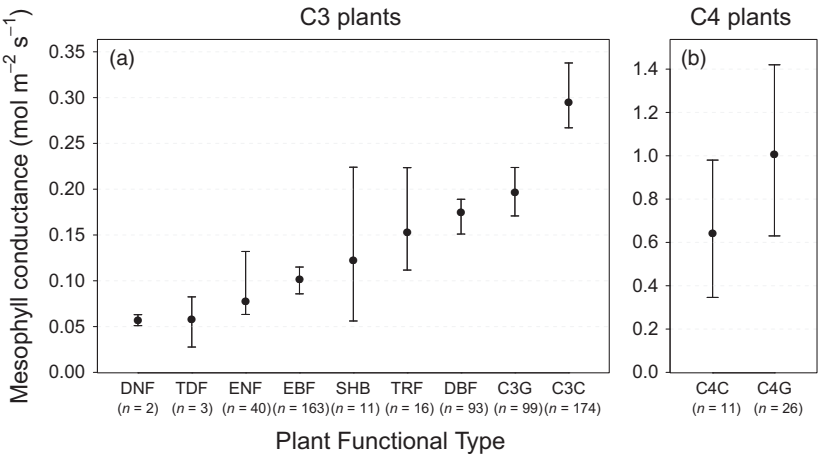

Figure 1. Maximum g_m values for the following plant functional types: DNF, deciduous needle-leaf trees; TDF, tropical deciduous trees; ENF, evergreen needle-leaf trees and shrubs; EBF, evergreen broadleaf trees and shrubs; SHB, deciduous shrubs; TRF, tropical evergreen trees; DBF, deciduous broadleaf trees; C3G, C3 grasses and herbs; C3C, C3 crops; C4G, C4 grasses and herbs; C4C, C4 crops. Dots and error bars represent medians and 95% confidence intervals of the median, respectively. Note the different scales in panels (a) and (b). Data are published values compiled by Knauer *et al.* (2019). In panel (b), additional data from the following studies are shown: Kolbe and Cousins (2018), Ubierna *et al.* (2018), Cano *et al.* (2019), and Zhou *et al.* (2019). All values were standardized to 25°C and processed as detailed in Knauer *et al.* (2019).

Flexas *et al.* (2018) for a literature review and Sun *et al.* (2014a) and Knauer *et al.* (2019) for a model-oriented review on these responses]. f_L reflects changes of leaf structure and associated decreases of maximum g_m within the canopy. Leaves that developed under higher light intensity (sun leaves) have a higher $g_{m,max25}$ than leaves that developed under lower light conditions (shade leaves), which has mainly been attributed to a higher S_c in sun leaves (Hanba *et al.*, 2002). Although responses of g_m to these environmental responses are well documented in the literature, the shapes of the response functions in Equation (6) are not well constrained and often differ widely across species and plant types (Galmés *et al.*, 2007; Warren *et al.*, 2007; von Caemmerer and Evans, 2015).

g_m has often been reported to respond to C_i (Flexas *et al.*, 2007; Hassiotou *et al.*, 2009; Xiong *et al.*, 2015), and light (Hassiotou *et al.*, 2009; Douthe *et al.*, 2012; Xiong *et al.*, 2018), but the physiological mechanisms behind these instantaneous responses remain elusive (see also Response of mesophyll conductance to environmental factors). The effects of C_i and light on g_m in a LSM have so far only been tested once by adding empirical response functions to Equation (6) (Figure 2d,e; Knauer *et al.*, 2019). Other factors such as salt stress (Delfine *et al.*, 1999; Wang *et al.*, 2018b) and ozone (Xu *et al.*, 2019) have been reported to negatively affect g_m instantaneously, but these stressors are not always considered in LSMs and have not yet been investigated with respect to g_m. On longer time scales (weeks to years) g_m is affected by nutrient availability (Jin *et al.*, 2011; Yamori *et al.*, 2011) and leaf age (Warren, 2006; Yin *et al.*, 2019). These factors have not been considered in g_m models incorporated in LSMs, but may be implemented in future applications, provided that available data can be translated into model functions.

Less information exists on the environmental responses of g_m in C4 plants, but new measurement techniques (Barbour *et al.*, 2016; Ubierna *et al.*, 2017) now enable investigation of these responses. Recent studies have indicated that C4 plants show similar responses as C3 plants with respect to temperature (Ubierna *et al.*, 2017), and C_i (Osborn *et al.*, 2017; Kolbe and Cousins, 2018; Ubierna *et al.*, 2018), as well as a similar decline with leaf age (Barbour *et al.*, 2016). These results suggest that the same model structure of g_m can be used for all photosynthetic pathways (Knauer *et al.*, 2019), however this suggestion still needs to be confirmed by future studies.

In LSMs, g_m is usually calculated *a priori* (e.g. Equation 6) and used to calculate C_c from Fick's first law (Equation 1). As also A_n depends on C_c, Equations (1) and (2) are usually solved in iterative loops, but analytical solutions also exist.

Adjustment of photosynthetic parameters

The adjustment of photosynthetic parameters is necessary if the implicit photosynthesis model is reformulated to account for g_m explicitly (i.e. if C_i is replaced by C_c in Equations 3 and 4). The adjustment affects all photosynthetic parameters, however, it is common practice to fix RuBisCO kinetic parameters (K_c, K_o, Γ^*) and adjust only photosynthetic capacity, as the former are assumed to be much less variable across C3 plants compared with V_{cmax} and J_{max} (Bernacchi *et al.*, 2009; but see Implications of the temperature response of mesophyll conductance). RuBisCO kinetic parameters and their temperature responses on a C_c basis have been, to the knowledge of the authors, so far only

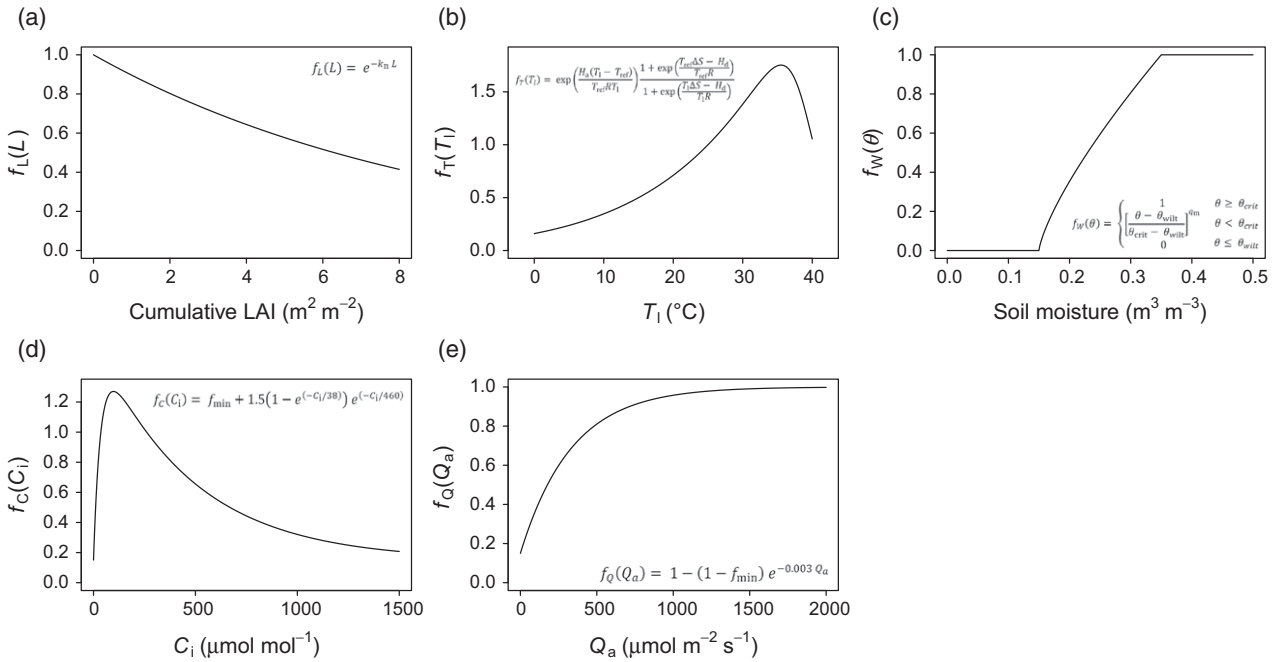

Figure 2. (a–c) Environmental response functions of g_m as shown in Equation (6). (d, e) Additional response functions as implemented in Knauer *et al.* (2019). L is the leaf area index (LAI), k_n is a within-canopy extinction coefficient (here k_n = 0.11), T_l is the leaf temperature, T_{ref} is the reference temperature (298.15 K), H_a is the activation energy, H_d is the deactivation energy, ΔS is the entropy term, R is the universal gas constant, θ is the volumetric soil moisture, θ_{wilt} is the soil moisture at the wilting point (here θ_{wilt} = 0.15 m^3 m^{-3}), θ_{crit} is the critical soil moisture (here θ_{crit} = 0.35 m^3 m^{-3}), q_m is the exponent determining the shape of the curve (here q_m = 0.75), C_i is the intercellular CO_2 concentration, f_{min} is the minimum g_m relative to $g_{m,max25}$ (here f_{min} = 0.15), and Q_a is the absorbed photosynthetic photon flux density. Parameters in (b) are taken from Bernacchi *et al.* (2002).

determined by two studies: Bernacchi *et al.* (2002), and Walker *et al.* (2013). From a theoretical point of view, both parameter sets are equally well suited for use in models. However, note that the choice of the RuBisCO kinetic parameters critically affects the adjustment of other parameters (see Implications of the temperature response of mesophyll conductance for a more detailed discussion) as well as the simulation of photosynthesis itself.

For the adjustment of V_{cmax} and J_{max}, two main approaches have been described (Sun *et al.*, 2014b; Knauer *et al.*, 2019). Both approaches fit the Farquhar *et al.* (1980) photosynthesis model to A_n–C_i curves *a priori* to the actual simulations but differ in several key aspects. The approach presented by Sun *et al.* (2014b) as applied by Sun *et al.* (2014a) employs a curve-fitting algorithm (Gu *et al.*, 2010), an extension of the approach proposed by Ethier and Livingston (2004), to estimate g_m, V_{cmax}, J_{max}, and the rate of TPU simultaneously from measured A_n–C_i curves. Sun *et al.* (2014b) fitted more than 1000 curves from almost 130 species from multiple plant types with or without a finite g_m. The fitted C_c-based V_{cmax}, J_{max}, and TPU were then related to their C_i-based counterparts using an empirical function (their Equation 4) with parameter-specific coefficients that allow the transformation from C_i-based to C_c-based values across plant types given that g_m and C_i-based parameter values are known. Knauer *et al.* (2019) make use of independently measured g_m values to convert simulated A_n–C_i curves under standard conditions (25°C and light saturation) to the corresponding A_n–C_c curves, to which V_{cmax} and J_{max} are fitted. The conversion is done for each PFT separately.

The use of simulated A_n–C_i curves as in Knauer *et al.* (2019) has the advantage that all model parameters as well as limitation states are known, and that the adjustment is applicable to different model structures (including C4 photosynthesis models) and values of the RuBisCO kinetic parameters. In contrast, the Sun *et al.* (2014b) method generates parameter estimates that are specific to the model structure as well as to the values of the RuBisCO kinetic parameters used, which limits transferability across models. For example, different coefficients have to be used for the monolimiting and colimiting versions of the Farquhar *et al.* (1980) model (Sun *et al.*, 2014a). One disadvantage of using simulated A_n–C_i curves as performed by Knauer *et al.* (2019) is that any model biases inherent in the implicit model are propagated to the C_c-based parameters.

Despite these differences, the two approaches give qualitatively similar parameter estimates for given combinations of g_m and C_i-based V_{cmax} and J_{max} (Figure 3). From Figure 3, three key aspects of the parameter adjustment become evident:

- **Higher C_c-based photosynthetic capacity:** C_c-based V_{cmax} and J_{max} compensate for the lower CO_2 concentration available for photosynthesis (C_c is always lower than C_i

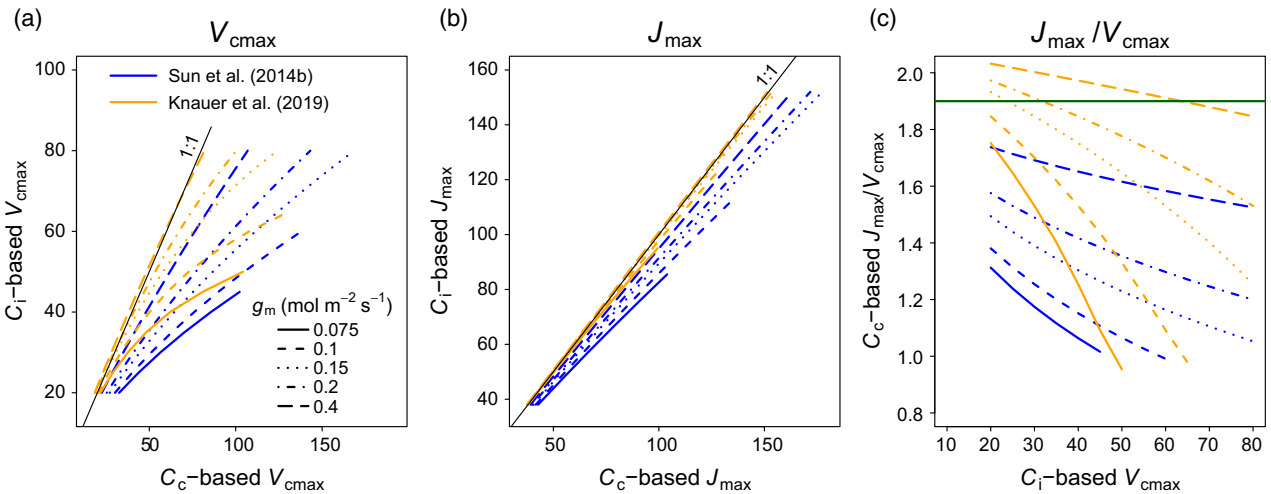

Figure 3. Comparison of the parameter adjustment from C_i-based to C_c-based values following Sun *et al.* (2014b), Equation (4) and Knauer *et al.* (2019) for (a) V_{cmax}, (b) J_{max}, and (c) J_{max}/V_{cmax} for different values of C_i-based V_{cmax}, J_{max}, and g_m (different line types). The apparent J_{max}/V_{cmax} ratio was assumed to be 1.9 (solid dark green line in (c)), and $R_l = 0.015 \cdot V_{cmax}$ for all simulations. Combinations of g_m and V_{cmax} that would lead to negative C_c values are not shown.

if A_n is positive) and are therefore generally higher than their C_i-based values (Figure 3a,b).

- **Asymmetric changes to V_{cmax} and J_{max}:** V_{cmax} are more strongly affected by the parameter adjustment than J_{max}. The effect of g_m on simulated photosynthesis is most pronounced when photosynthesis is most sensitive to C_i, which is usually in the RuBisCO (V_{cmax})-limited domain (Equation 3) and under low C_i. For the same reason, TPU is less affected than J_{max} (Sun *et al.*, 2014b).
- **Adjusted parameters depend on both g_m and photosynthetic capacity:** the effects of the adjustment are most pronounced when g_m has a strong effect on the available CO_2 concentration. Thus, C_c-based parameters will differ more strongly from their C_i-based values when the C_i–C_c drawdown is high, which is the case if g_m is low and/or V_{cmax} is high.

In addition to these key changes, the derived C_c-based parameter values depend on several other factors. Most importantly, the assumed values of the RuBisCO kinetic parameters cause most of the differences between the two approaches. The relationship between C_i-based and C_c-based values is also affected by the J_{max}/V_{cmax} ratio, R_l, the C_i-range of the curves, and the structure of the photosynthesis model in general. Hence, a strict correspondence of adjusted parameter values cannot be expected across methods. Nonetheless, future work needs to resolve the reasons for the striking quantitative differences in the derived V_{cmax} and J_{max} values between the two approaches (Figure 3). A_n–C_i curves will provide the most important constraints for the validation of the adjusted parameters. As stated above, the inclusion of g_m into models should not lead to strong deviations in simulated A_n–C_i curves. In particular at high C_i, when photosynthesis is CO_2-saturated, the g_m-implicit and the g_m-explicit curves must not show a significant offset.

EFFECTS OF MESOPHYLL CONDUCTANCE IN LAND SURFACE MODEL SIMULATIONS

Changes to A_n–C_i curves

The effects that physiological processes have on water and carbon fluxes at larger spatial scales are predominantly determined by how they are represented at the leaf level. Therefore, before turning to the consequences of an explicit representation of g_m for large-scale water and carbon fluxes, we first investigate its implications for leaf-level photosynthesis. We explore the effects of g_m on leaf gas exchange with the help of A_n–C_i curves, which are commonly used to characterize fundamental physiological properties of leaves (Farquhar and Sharkey, 1982; Long and Bernacchi, 2003) An intuitive way of demonstrating the effects of g_m is of thinking about the ways that it reduces the available CO_2 concentration for photosynthesis, which shifts the operating point lower down (i.e. to a steeper part of) the curve, thereby increasing the CO_2 responsiveness of photosynthesis (Niinemets *et al.*, 2011). While it is true that the presence of a finite g_m reduces C_c relative to C_i, this reduction does not necessarily lead to simulated changes in the CO_2 sensitivity of photosynthesis, because other photosynthetic parameters in the model are also adjusted to match the A_n–C_i curve and thus largely compensate for the lower available CO_2 concentration (see Adjustment of photosynthetic parameters). This needs to be the case because A_n–C_i curves represent measured values independent of the values of g_m (i.e. they implicitly include effects of g_m). Consequently, both C_i-based and

C_c-based models aim to fit the same measurements (A_n–C_i curves) as closely as possible. Nonetheless, the explicit and implicit models will not simulate exactly the same A_n–C_i curves. Several characteristic differences in fitted and simulated A_n–C_i curves emerge (Figure 4):

1. Transition point at lower C_i: A_n–C_i curves modelled by the explicit model show an earlier transition point (sometimes referred to as inflection point) from RuBisCO-limited photosynthesis at low C_i (Figure 4) to RuBP regeneration-limited photosynthesis at higher C_i. The shift in the transition point is the result of the lower J_{max}/V_{cmax} ratio in the explicit model (Figure 3), which is required to match A_n–C_i curves. An earlier transition point also means that photosynthesis is more often limited by RuBP regeneration (Equation 4), which shows a lower sensitivity to increases in CO_2 compared with the RuBisCO-limited domain (i.e. lower slope in Figure 4).

2. Smoother A_n–C_i curves: a finite g_m changes the curvature of A_n–C_i curves and leads to smoother curves (Ethier and Livingston, 2004). From Figure 4 it is apparent that this is mostly caused by the part of the curve that is limited by RuBP regeneration and close to the transition point.

3. Different temperature and light sensitivities: this effect is not evident from A_n–C_i curves measured at standard conditions (25°C and saturating light), and is therefore often overlooked in studies of g_m. The clear temperature response of g_m (Figure 2b) causes substantially different curves under lower and higher temperatures and, to a lesser extent, also at subsaturating light intensities (Figure 4). This effect is responsible for most of the differences found between the g_m-implicit and g_m-explicit simulations (Effects on global carbon and water fluxes) but is also subject to considerable uncertainties which are discussed in more detail in Implications of the temperature response of mesophyll conductance.

The strength of these effects generally increases with decreasing g_m and therefore differ among plant types (Figure 1).

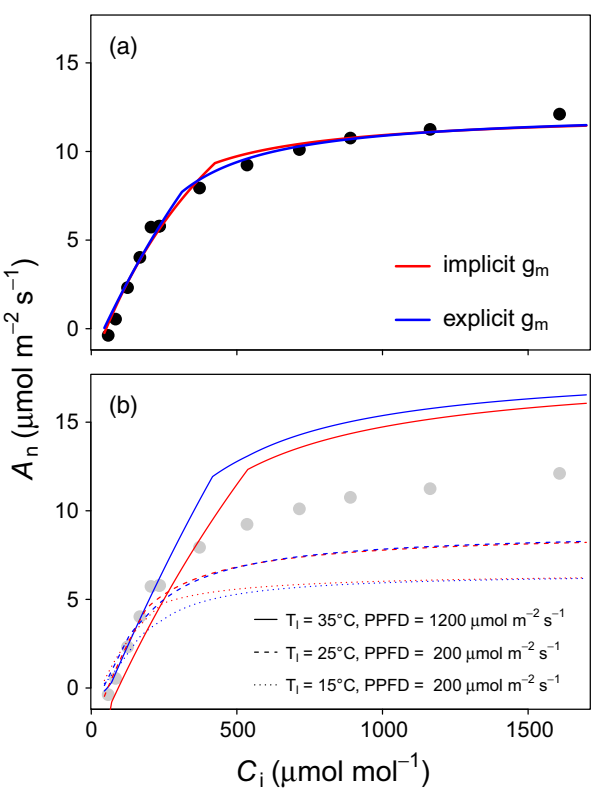

Figure 4. (a) A_n–C_i curve (dots) fitted with the *plantecophys* R package (Duursma, 2015) with and without a finite g_m. The A_n–C_i curve was measured for *Pinus pinaster* at 23°C and 1200 µmol m^{-2} sec^{-1} photosynthetic photon flux density (PPFD) and is available from Kumarathunge *et al.* (2018), curve number 3888. g_m and R_l at 25°C were assumed to be 0.1 mol m^{-2} sec^{-1} and 0.56 µmol m^{-2} sec^{-1}, respectively. The derived parameters at 25°C from the curve fits are: $V_{cmax25,ci}$ = 30.98 µmol m^{-2} sec^{-1}, $V_{cmax25,cc}$ = 38.25 µmol m^{-2} sec^{-1} $J_{max25,ci}$ = 58.94 µmol m^{-2} sec^{-1}, $J_{max25,cc}$ = 59.02 µmol m^{-2} sec^{-1}, in which the subscripts $_{ci}$ and $_{cc}$ denote C_i-based and C_c-based, respectively. TPU limitation was not present in either of the two curves. (b) simulated A_n–C_i curves for the same parameters as derived from the curves shown in panel (a) but at contrasting leaf temperatures (T_l) and light conditions. The same points as in panel (a) are shown for orientation. Temperature responses of the parameters are taken from Bernacchi *et al.* (2001, 2002, 2003).

Effects on global carbon and water fluxes

The changes to A_n–C_i curves as described in the previous section suggest that the effects of g_m will be most pronounced in regions that are covered by vegetation with low g_m (e.g. boreal forests), and that are characterized by meteorological conditions that deviate strongly from the temperature and light conditions at which A_n–C_i curves are routinely measured. These presumptions were confirmed in the two studies that investigated the global implications of replacing the implicit g_m with an explicit representation (Sun *et al.*, 2014a; Knauer *et al.*, 2019). The effects of g_m on GPP, ET, and transpiration between the two studies is compared in Figure 5. Note that absolute values between the two studies are not directly comparable as simulation periods, and thus CO_2 and climate effects, differed. With respect to GPP, two key results become evident from Figure 5: first, GPP increases more strongly in simulations where g_m is simulated explicitly, and second, the effect of g_m on GPP shows a clear latitudinal pattern with higher effects on GPP in the extratropical zone compared with the tropics. Strongest effects were consistently found in the boreal and subarctic zones (50–70°) and intermediate effects in the temperate zone of both hemispheres. Notwithstanding these general agreements, some differences between the two studies can be identified. Most importantly, the effects of g_m on GPP are negative in the inner tropics in the simulations conducted by Knauer *et al.* (2019), whereas they remain positive throughout all latitudes and comparatively high around the equator in the simulations by Sun *et al.* (2014a).

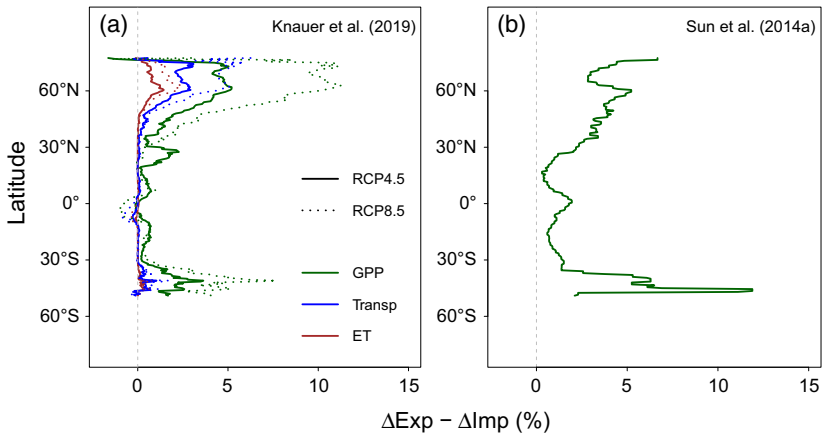

Figure 5. Effects of g_m on gross primary productivity (GPP), transpiration (Transp), and evapotranspiration (ET) for simulations by (a) Knauer *et al.* (2019) (model versions 'Imp' and 'Exp') and (b) Sun *et al.* (2014a)(GPP only). Δ is defined as $\Delta = (F_{t2} - F_{t1})/F_{t1}$, where F_{t1} and F_{t2} are mean annual fluxes averaged for time periods t1 and t2, respectively. 'Exp' and 'Imp' denote g_m-explicit and g_m-implicit model simulations, respectively. Positive values indicate higher fluxes in the g_m-explicit model simulations compared with the g_m-implicit simulations, negative values the opposite. Note that t1 and t2 are different for the two studies [Knauer *et al.* (2019): t1 = 1975–2004, t2 = 2070–2099 (RCP scenarios); Sun *et al.* (2014a): t1 = pre-industrial, t2 = 1981–2010], hence absolute values are not directly comparable.

The responses seen in Figure 5 are the combined effects of vegetation types and the prevailing meteorological conditions. As described in Changes to A_n–C_i curves, g_m causes a higher fraction of photosynthesis to be RuBP-limited (Equation 4), which shows a lower CO_2 sensitivity than the RuBisCO-limited domain (Equation 3). However, this is offset by higher CO_2 sensitivities in the g_m-explicit model under a wide range of (especially low) temperatures and CO_2 concentrations (Figure 4), resulting in an overall higher photosynthetic CO_2 sensitivity in the g_m-explicit simulations. In addition, the effects of g_m on simulated photosynthesis are strongest when its magnitude is low. Hence, effects of g_m are most pronounced in the boreal zone, where needle-leaf evergreen forests with a low g_m grow in a comparatively cold climate in which g_m-explicit photosynthesis shows the highest CO_2 sensitivity (Figure 4). g_m did not have any effects on simulated GPP and transpiration in C4 plants in the JSBACH simulations performed by Knauer *et al.* (2019), but these results still need to be confirmed by other modelling studies.

The effects of g_m on transpiration in the simulations by Knauer *et al.* (2019) follow those of GPP, but have lower magnitudes. The close agreement in the effects of g_m on GPP and transpiration results from the close coupling between carbon and water fluxes at the leaf level in LSMs (see also Mesophyll conductance and water-carbon coupling). In JSBACH model simulations, g_s was simulated with the model by Medlyn *et al.* (2011), in which changes in A_n also affect g_s and thus transpiration. The fact that transpiration is significantly less affected by g_m than A_n is because first, g_m effects on g_s, and thus transpiration, are only indirect via the effects of g_m on A_n, second, because a small fraction of stomatal conductance (the g_0 parameter representing the residual g_s) is unaffected by changes in A_n, and third, because changes in g_s do not translate into the same fractional changes in transpiration due to canopy-atmosphere decoupling (McNaughton and Jarvis, 1991; De Kauwe *et al.*, 2013; Knauer *et al.*, 2017). Likewise, ET is even less affected by changes in g_m, as it consists of a varying fraction of water fluxes (evaporation) that are independent of leaf physiological processes. Note that all these model feedbacks vary widely across models (e.g. the fraction of transpiration on ET varies from 20 to 60% in LSMs; Wei *et al.*, 2017), therefore the actual effects of g_m on water fluxes are likely to be highly model specific.

The two climate scenarios shown in Figure 5(a) show very similar latitudinal patterns, but significantly stronger effects for both water and carbon fluxes in the RCP8.5 scenario, which assumes significantly higher CO_2 concentrations and temperatures at the end of the 21st century compared with the RCP4.5 scenario.

The altered responses of carbon and water fluxes (Figure 5) have important consequences for simulations of biogeochemical and biophysical fluxes in the Earth system. Implications of these changes are most relevant for the carbon cycle. Knauer *et al.* (2019) found an additional mean annual gross carbon uptake of 2.3–6.6 PgC year^{-1} in the g_m-explicit simulations for the 2070–2099 period. In the simulations conducted by Sun *et al.* (2014a), the consideration of g_m led to an additional 142 PgC gross uptake over the 1901 to 2010 time period, which in 2010 was equivalent to *c.* 17 ppm of additional atmospheric CO_2. These numbers suggest that the capacity of terrestrial ecosystems for carbon uptake is underestimated in current LSMs, and that the lack of g_m might contribute to the overestimation of

the growth rate of atmospheric CO_2 by LSMs (Sun *et al.*, 2014a). g_m might also play a role in the long-term trends in the seasonal amplitude of atmospheric CO_2. The cause for this increase has been attributed primarily to the role of GPP (Forkel *et al.*, 2016), but the physiological basis for this increased photosynthetic activity has not yet been investigated. It is likely that g_m plays a role in the growth of the seasonal amplitude of CO_2 because its effects are strongest in the extratropical northern hemisphere (Figure 5), the region in which the growth of the CO_2 seasonal amplitude is most pronounced (Forkel *et al.*, 2016). However, more work is needed to assess the role of plant physiology in general, and g_m in particular, in the enhanced seasonal CO_2 exchange.

Changes in ET, although less pronounced than those for GPP, also cause changes in the simulated large-scale water cycle. A stronger increase in ET (Figure 5a) involves changes in surface hydrology, including decreases in run-off and continental discharge (Gedney *et al.*, 2006; Knauer *et al.*, 2017), but also decreases in surface temperature and associated climate feedbacks (Boucher *et al.*, 2009). Although these feedbacks are relatively well understood, the biophysical consequences of an explicit representation of g_m in LSMs still need to be investigated.

Mesophyll conductance and water-carbon coupling

The diffusion pathway for CO_2 into the leaf is affected by both g_s and g_m, whereas water vapour flux out of the leaf is only affected by g_s. Therefore, it can be expected that intrinsic water-use efficiency (iWUE = A_n/g_s) decreases when the g_m/g_s ratio decreases (Flexas *et al.*, 2013a, 2016). In LSMs, iWUE is commonly determined by models that relate g_s linearly to A_n for a given atmospheric environment (Ball *et al.*, 1987; Leuning, 1995; Medlyn *et al.*, 2011). These formulations do not permit A_n and g_s to change independently and force C_i/C_a to remain constant with increasing C_a under the same atmospheric humidity. A constant C_i/C_a is associated with a proportional increase of iWUE with C_a, a behaviour that is well supported by data (Ainsworth and Long, 2005; De Kauwe *et al.*, 2013; Franks *et al.*, 2013; Frank *et al.*, 2015). However, this model behaviour contradicts the expected relationship between g_m/g_s and iWUE (Flexas *et al.*, 2013a), as iWUE in LSMs is not predicted to change even if g_m/g_s is changing, because any effects of g_m on A_n are compensated for by changes in g_s in the opposite direction to keep C_i/C_a constant (Knauer *et al.*, 2019). Additionally, the described changes in g_s and transpiration with an explicit g_m (Effects on global carbon and water fluxes) are not direct effects of g_m, but indirect consequences of the behaviour of stomatal models used in LSMs. Future work needs to resolve the contrasting evidence for the effects of g_m on iWUE, which is relevant for the representation of water-carbon coupling in models.

Mesophyll conductance and soil water stress

When exposed to soil water stress, plants reduce g_m, which limits photosynthesis along with other diffusional (i.e. stomatal) and biochemical limitations (photosynthetic capacity) (Grassi and Magnani, 2005; Galmés *et al.*, 2007; Varone *et al.*, 2012; Zhou *et al.*, 2014; Nadal and Flexas, 2018). The explicit representation of g_m in models therefore allows to account for an additional mechanism to downregulate vegetation activity under water stress. Soil water stress in LSMs is usually represented as a simple scalar (Figure 2c), which reduces A_n and/or g_s as a function of soil moisture (Egea *et al.*, 2011; Verhoef and Egea, 2014). Egea *et al.* (2011) showed with simulation experiments that observed water stress-induced decreases in A_n, g_s, and iWUE are not well captured by simulating decreases in A_n and/or g_s only, but simulations could be improved when either decreases in g_s and g_m were taken into account, or when all three factors were downregulated simultaneously. Similarly, Keenan *et al.* (2010) found that applying a combination of g_s and g_m response functions could adequately simulate plant drought responses in a Mediterranean oak ecosystem. Despite the widespread evidence of increasing diffusional limitations under water stress, the consideration of g_m as an additional diffusional limitation into models does not necessarily improve simulated drought responses of vegetation. Zhou *et al.* (2013) concluded that observed decreases in C_i-based V_{cmax} under water stress could be caused by decreases in either g_m or V_{cmax}, and Keenan *et al.* (2010) also concluded that biochemical limitations alone could adequately capture vegetation drought responses. In light of this high degree of equifinality, it appears likely that the inclusion of g_m as an additional mechanism to the downregulation of A_n (and g_s) can only improve simulations of water stress responses in LSMs if it is carefully parameterized.

Mesophyll conductance and carbon isotope discrimination

Models describing the discrimination of ^{13}C isotopes during photosynthesis allow important insights into gas exchange characteristics of plants (Farquhar *et al.*, 1982). Photosynthetic discrimination models differ in their complexity, depending on the number of fractionation processes considered (see e.g. Ubierna and Farquhar, 2014 for an overview). Most commonly, a simple discrimination model is used, which accounts for fractionation by stomata and RuBisCO only. Knowledge of g_m (and thus C_c) allows us also to consider fractionation associated with leaf internal CO_2 transport. Importantly, the more comprehensive photosynthetic discrimination model gives a different eco-physiological interpretation of the same $\delta^{13}C$ data than the simple model (Wingate *et al.*, 2007; Seibt *et al.*, 2008; Ubierna and Farquhar, 2014).

In LSMs, g_m is relevant for forward simulations of carbon isotope ratios in terrestrial vegetation (Suits *et al.*, 2005) that can provide important insights on the spatial and temporal dynamics of terrestrial carbon sources and sinks (Scholze *et al.*, 2008) and WUE (Peters *et al.*, 2018). The role of g_m in large-scale simulations of carbon isotope discrimination has recently been investigated by Keeling *et al.* (2017), who found that the observed decreasing trend in atmospheric $\delta^{13}C$ could only be explained if carbon isotope fractionation caused by g_m was considered in the photosynthetic discrimination model. In that study, a (relatively high) constant global mean value of g_m was assumed. A spatially and temporally explicit representation of g_m is likely to enhance the ability of LSMs to simulate continental fluxes of ^{13}C and provide better large-scale constraints on vegetation water-carbon coupling.

CHALLENGES AND PATHWAYS FOR MODEL IMPROVEMENT

Studies implementing g_m into LSMs have found that the explicit representation of g_m changes the response of simulated photosynthesis to environmental factors. This includes changing temperature and CO_2 sensitivities of photosynthesis, which has far-reaching implications for simulations of large-scale carbon and water fluxes in LSMs (Sun *et al.*, 2014a; Knauer *et al.*, 2019). In the following section, we present several key uncertainties in global models of g_m and how future model developments may contribute to better represent the effects of g_m on present and future global flux simulations.

Magnitude of mesophyll conductance across plant types

The explicit representation of g_m in LSMs requires that the magnitude of g_m can be sufficiently well determined across plant types, as its effects on photosynthesis depend strongly on its magnitude (Changes to A_n–C_i curves). This is hampered because measurements of g_m are challenging, in particular because the calculated absolute values are sensitive to assumptions on several input variables such as Γ^* and R_l (Pons *et al.*, 2009). Nevertheless, despite these inherent high uncertainties in individual measurements, compilations of g_m values (Flexas *et al.*, 2008; Nadal *et al.*, 2018; Figure 1), can provide relatively robust estimates of the magnitude of g_m (confidence intervals in Figure 1) that are suitable for use in LSMs (e.g. as $g_{m,max25}$ in Equation 6). While this seems to be the case for well studied PFTs, more measurements are needed for deciduous needle-leaf trees, tropical trees (both deciduous and evergreen), as well as C4 plants. The magnitude of g_m in other plant groups such as bryophytes and ferns is relatively well constrained and lower compared with those shown in Figure 1 [bryophytes: 0.005 ± 0.004 mol m^{-2} sec^{-1} (median $\pm$ standard error of the median), ferns: 0.05 ± 0.013 mol m^{-2} sec^{-1} (Gago *et al.*, 2019)]. These plant groups are usually not considered in LSMs, despite their potentially significant contributions to terrestrial carbon uptake, especially at higher latitudes (Sjögersten *et al.*, 2006; Turetsky *et al.*, 2012). Future model developments that aim to include ferns and bryophytes into models will need to take g_m into account as an important physiological determinant in these plant groups.

Predicting maximum mesophyll conductance from other plant properties

The importance of knowing the magnitude of g_m for simulations of photosynthesis and transpiration emphasizes the need to predict the key parameter $g_{m,max25}$, the maximum g_m at 25°C (Equation 6), from more readily available plant traits. g_m shows a strong relationship with photosynthetic capacity and thus A_n (Evans and Von Caemmerer, 1996; Hanba *et al.*, 2001; Douthe *et al.*, 2012; Ouyang *et al.*, 2017), and it follows from first-order principles (Equation 1) that g_m and photosynthetic capacity have to be correlated to some extent, as for example high photosynthetic rates can only be achieved if g_m is high enough to allow the supply of sufficient CO_2 to the sites of carboxylation. However, g_m is unlikely to be determined from a CO_2 supply-demand aspect only because plants are subject to additional structural constraints that affect g_m but not directly photosynthetic capacity. In fact, the A_n–g_m or V_{cmax}–g_m relationships are not conserved across species (Ethier and Livingston, 2004; Warren, 2008b).

A co-regulation between g_m and leaf hydraulic conductance (K_{leaf}) has been suggested based on the fact that CO_2 and water share parts of the diffusion pathway in the leaf mesophyll (Flexas *et al.*, 2013b). However, a close relationship between g_m and K_{leaf} could not always be found (Loucos *et al.*, 2017; Wang *et al.*, 2018a). Furthermore, a strong coordination between g_m and K_{leaf} cannot be expected due to the fact that K_{leaf} includes pathways such as the xylem that do not play a role for leaf internal CO_2 transfer (Flexas *et al.*, 2013b). g_m often shows a good correlation with g_s (Lauteri *et al.*, 1997; Jin *et al.*, 2011), but the mechanistic relationship between these two variables is unclear. In fact, the correlation between g_s and g_m may be spurious as g_s is also strongly correlated with A_n, which is more directly linked to g_m (Equation 1).

g_m has been related to several leaf anatomical traits. One trait integrating several leaf anatomical properties is specific leaf area (SLA = leaf area/leaf dry weight). Despite good relationships across species (Niinemets *et al.*, 2009), this trait does not always explain a significant variation in g_m (Nadal *et al.*, 2018; Xiong and Flexas, 2018). Importantly, SLA is unlikely the most suitable trait for predicting $g_{m,max25}$ as it integrates several leaf properties that may have contrasting effects on g_m (Niinemets *et al.*, 2009; Onoda *et al.*, 2017). For example, a lower SLA (i.e. heavier leaves for the

same leaf area) could be caused by thicker cell walls, which tend to decrease g_m, or by increased leaf thickness and associated higher S_c, which tend to increase g_m. The relationship between other leaf anatomical traits (e.g. cell wall thickness, S_c) and g_m have been investigated for various species (Evans *et al.*, 1994; Tomás *et al.*, 2013; Peguero-Pina *et al.*, 2017; Veromann-Jürgenson *et al.*, 2017; Xiong *et al.*, 2017), but still need to be determined across plant types.

Given the complex nature of g_m and its dependence on various anatomical and physiological factors, it is unlikely that a single plant trait can explain a significant variation in g_m. We therefore suggest that a combination of properties related to photosynthetic capacity (e.g. A_n, V_{cmax}, leaf N) and anatomical traits need to be considered to predict maximum g_m across plant types.

Response of mesophyll conductance to environmental factors

In addition to the magnitude of g_m, models need to capture variations of g_m with changes in the environment. The response of g_m to environmental factors is generally subject to substantial uncertainties that arise from the fact that the quality of the response of g_m to environmental factors (i.e. the actual shape of the response curves shown in Figure 2) varies strongly across species or PFTs. For example, while it is uncontested that g_m responds to soil water stress and temperature, the shapes of the responses differ widely across studies and species. Likewise, the gradient of g_m across the canopy varies across studies (Warren *et al.*, 2007; Montpied *et al.*, 2009; Han *et al.*, 2010; Cano *et al.*, 2011; Zhang and Yin, 2012). Future efforts should compare existing measurements in a systematic manner. Comparing measurements in the context of the parameter values in formulations that are directly usable in LSMs (e.g. the light extinction coefficient k_n in Figure 2a) can give important insights as to whether these formulations are applicable across PFTs.

Uncertainty is also caused by the role of environmental factors, foremost C_i and light, whose effects on g_m are still under debate. Most studies investigating these responses have found that g_m decreases with C_i (Flexas *et al.*, 2007; Hassiotou *et al.*, 2009; Vrábl *et al.*, 2009; Xiong *et al.*, 2015; Moualeu-Ngangue *et al.*, 2017) and increases with light (Hassiotou *et al.*, 2009; Douthe *et al.*, 2012; Xiong *et al.*, 2018), although exceptions exist for both the C_i (Tazoe *et al.*, 2009; Pengelly *et al.*, 2014) and light response (Tazoe *et al.*, 2009; Yamori *et al.*, 2010; Loucos *et al.*, 2017). A major complication with these observations is that their mechanistic basis is still unknown (Carriquí *et al.*, 2019 and references therein) as well as that they may be artefactual. Gu and Sun (2014) demonstrated that both the C_i and light response of g_m may be caused by various methodological factors such as unreliable R_l and Γ^* estimates or positively biased C_i measurements. In addition, it has been suggested that the presence of a light response of g_m in measurements may be apparent, as the extent to which different cell layers within the leaf contribute to the total g_m vary with light intensity (Théroux-Rancourt and Gilbert, 2017).

The C_i and light responses of g_m at the leaf level are critical for the implications of an explicit representation of g_m for carbon and water fluxes at the global scale. The presence of a C_i response would have to be accounted for when parameters are adjusted using A_n–C_i curves (see Adjustment of photosynthetic parameters), i.e. g_m would have to be assumed to vary with C_i. This would affect the parameter adjustment and lead to different C_c-based V_{cmax} and J_{max} values, but would not lead to significant changes in global simulations of GPP and transpiration (Knauer *et al.*, 2019). In contrast, a potential light response of g_m at leaf level would be amplified at canopy and larger spatial scales as leaves in the lower canopy continuously operate at low light. Upscaled to the global scale, a g_m responding to light would result in significantly stronger responses of both GPP and transpiration in all major biomes (Knauer *et al.*, 2019).

Multiplicative models (e.g. Equation 6) are able to modify g_m to an optional number of environmental factors, but have the drawback of not being able to account for interactions among variables, which are likely to exist in the case of g_m (Xiao and Zhu, 2017). In addition, multiplicative formulations can be difficult to parameterize as they contain many empirical parameters that often lack a clear biological meaning. Given these drawbacks, future model development should overcome the use of multiplicative equations and head towards simpler formulations accounting for interactive effects among key variables. The representation of g_m separated into chloroplast and cell wall components and therefore accounting for two different compartments acting as CO_2 sinks (chloroplasts) and sources (mitochondria) (Tholen *et al.*, 2012) could improve the representation of g_m in models, but suffers from the key limitation that measurements of the individual components of g_m are not available in most cases.

Implications of the temperature response of mesophyll conductance

A significant effect of the differences between g_m-implicit and g_m-explicit model simulations at the global scale come from the fact that the temperature sensitivity of photosynthesis changes when g_m is simulated explicitly (see Figure 4b). These results are mainly the effect of the strong temperature response of g_m itself that is employed in global models. This temperature response (Bernacchi *et al.*, 2002; Figure 2b) was measured for the (sub)tropical species *Nicotiana tabacum* (tobacco) and is therefore unlikely to adequately represent temperature responses in other plant types or climate zones. However, for modelling purposes it is not acceptable to simply replace the temperature response function of *N. tabacum* with those of other

species. The reason for this is that the temperature function of g_m was derived in tandem with the temperature response of C_c-based RuBisCO kinetic parameters (K_c, K_o, Γ^*), which means that the latter are only valid in combination with that particular temperature response function. Using RuBisCO kinetic parameters and temperature-response functions from different sources (i.e. parameter 'mixing and matching') is bad modelling practice, which should be avoided whenever possible (Rogers *et al.*, 2017).

In addition to these theoretical modelling considerations, a few further complications exist. One is that temperature responses of g_m vary considerably across species. von Caemmerer and Evans (2015) found widely differing temperature responses across species that could not be explained by plant types or climatic origin. A second complication is that RuBisCO kinetic parameters may also not be as constant across C3 plants as they are commonly assumed to be. In a compilation of C_i-based Michaelis-Menten constants, Galmés *et al.* (2016, 2019) reported differences that could be related to the climate origin of the species. The few measurements that exist of C_c-based K_c and K_o temperature responses also indicate huge differences between species. For example, RuBisCO kinetic parameters of *Arabidopsis thaliana* showed a much weaker temperature response than *N. tabacum* (Walker *et al.*, 2013). To better constrain this key uncertainty, the following analyses are suggested:

- Measurement of RuBisCO kinetic parameters, g_m and their temperature responses for the same set of leaves in different plant types or under different growth conditions: this analysis could reveal whether differences in the measured temperature response of g_m are in fact caused by differences in the temperature response of RuBisCO kinetic parameters. Comprehensive measurements as done by Bernacchi *et al.* (2002) and Walker *et al.* (2013) for contrasting species would provide parameter values that can directly be used in LSMs.
- Fitting of A_n–C_i curves under different temperatures with and without an explicit g_m: If the strong temperature response of g_m holds across species in different growth environments, the consideration of g_m (and its temperature response) in curve-fitting algorithms should result in better fits to A_n–C_i curves particularly under low and high temperatures. Therefore, future A_n–C_i curve analysis must focus on measurements under non-ideal temperature and light conditions.

Acclimation of mesophyll conductance to the environment

None of the modelling approaches described in this review has considered the possibility that g_m may acclimate (i.e. adjust physiologically or anatomically) to changes in the growth environment such as CO_2 concentration or temperature (but note that f_L in Equation 6 accounts for acclimation to growth irradiance). It has been suggested that plants grown under elevated CO_2 may exhibit a reduced g_m due to increased starch accumulation or thicker cell walls (Nakano *et al.*, 2000; Sawada *et al.*, 2001; Shrestha *et al.*, 2019; Mizokami *et al.*, 2019b). However, studies in which plants were grown under different CO_2 concentrations did not show consistent differences in g_m measured at the same CO_2 concentration. Singsaas *et al.* (2003) found reductions in g_m for some species, but increases in others, Kitao *et al.* (2015) found a decreased g_m only under N limiting conditions, and Mizokami *et al.* (2019a) determined slight, statistically insignificant, increases in g_m for *A. thaliana* plants grown under elevated CO_2. Mizokami *et al.* (2019b) found lower g_m under elevated growth CO_2 which could be attributed to thicker cell walls, whereas Shrestha *et al.* (2019) could not identify a lower g_m with decreases in cell wall thickness. Clearly, more experiments are needed in which g_m as well as leaf anatomical traits are determined in plants grown under different CO_2 concentrations. Given that g_m measurements themselves are often affected by CO_2 concentrations, gas exchange measurements aiming to resolve acclimation effects should be performed under the same atmospheric or, ideally, intercellular CO_2 concentrations.

Acclimation of g_m to temperature has been investigated in only a few studies. In some cases, optimum temperatures for g_m depended on the growth temperature of the plants, with a lower optimum associated with lower growth temperatures (Yamori *et al.*, 2006; Silim *et al.*, 2010), effects that have been attributed to the role of proteins (CA and cooporins) in leaf internal CO_2 transfer, or to leaf anatomical adjustments. These effects have not been found in other studies (Warren, 2008a; Dillaway and Kruger, 2010), however in these studies acclimation was also absent in other photosynthetic parameters.

Temperature acclimation has been more comprehensively and systematically assessed for other photosynthetic parameters like dark respiration (Atkin *et al.*, 2015) or V_{cmax} and J_{max} (Kattge and Knorr, 2007; Kumarathunge *et al.*, 2019). In these studies, model formulations have been derived that allow the implementation of acclimation into LSMs. Accounting for photosynthetic acclimation in LSMs affected projections of the global carbon cycle (Smith *et al.*, 2016) and associated biophysical climate feedbacks (Smith *et al.*, 2017). From a modelling point of view, the existence of acclimation would require the adjustment of $g_{m,max25}$ (Equation 6) depending on growth conditions. Unfortunately, there is currently no means to implement and assess effects of a possible temperature acclimation of g_m at larger scales explicitly. Temperature acclimation of photosynthetic capacity has been performed with C_i-based parameter values that implicitly contain information on any possible acclimation of g_m. Hence, acclimation effects of C_c-based V_{cmax} and J_{max} values will be different if g_m shows either a different temperature response across

species, or acclimation itself (Yamori *et al.*, 2006; Warren, 2008a; Dillaway and Kruger, 2010).

CONCLUSIONS

Mesophyll conductance is, to date, mostly ignored in LSMs because parameters in current photosynthesis models have been optimized to use C_i instead of C_c as the available CO_2 concentration for carboxylation. This is despite a growing number of measurements that can be used to constrain the magnitude of g_m across plant types, represent its variation with environmental conditions, and re-calibrate model parameters on a C_c basis. Recent modelling approaches incorporating this information into LSMs indicate that an explicit g_m leads to altered environmental responses of photosynthesis, which result in increased climate and CO_2 sensitivities of GPP and transpiration particularly in the boreal zone. Future efforts should aim to reduce model uncertainties associated with the response of g_m to light and temperature as well as to improve current formulations of g_m by accounting for interactions among variables and by employing fewer, but biologically meaningful, parameters.

ACKNOWLEDGEMENTS

MDK acknowledges support from the ARC Discovery Grant (DP190101823), the Australian Research Council Centre of Excellence for Climate Extremes (CE170100023) and the NSW Research Attraction and Acceleration Programme.

AUTHOR CONTRIBUTIONS

JK designed this review and wrote the original draft; YS provided model simulation results; SZ, MDK, VH, MR, and YS provided ideas and comments on the first draft and helped writing the manuscript.

CONFLICT OF INTEREST

The authors declare no conflict of interest.

DATA AVAILABILITY STATEMENT

Code for the parameter adjustment (Figure 3) and land surface model simulation results (Figure 5) are available from https://bitbucket.org/juergenknauer/mesophyll_conductance.

REFERENCES

Ainsworth, E.A. and Long, S.P. (2005) What have we learned from 15 years of free-air CO_2 enrichment (FACE)? A meta-analytic review of the responses of photosynthesis, canopy properties and plant production to rising CO_2. *New Phytol.* **165**, 351–372.

Atkin, O.K., Bloomfield, K.J., Reich, P.B. *et al.* (2015) Global variability in leaf respiration in relation to climate, plant functional types and leaf traits. *New Phytol.* **206**, 614–636.

Ball, J.T., Woodrow, I.E. and Berry, J.A. (1987) A model predicting stomatal conductance and its contribution to the control of photosynthesis under different environmental conditions. In *Progress in Photosynthesis Research* (Biggins, J. ed). Dordrecht, Netherlands: Martinus Nijhoff Publishers, pp. 221–224.

Barbour, M.M., Evans, J.R., Simonin, K.A. and Caemmerer, S. (2016) Online CO_2 and H_2O oxygen isotope fractionation allows estimation of mesophyll conductance in C4 plants, and reveals that mesophyll conductance decreases as leaves age in both C4 and C3 plants. *New Phytol.* **210**, 875–889.

Bernacchi, C.J., Singsaas, E.L., Pimentel, C., Portis, A.R. Jr and Long, S.P. (2001) Improved temperature response functions for models of Rubisco-limited photosynthesis. *Plant, Cell Environ.* **24**, 253–259.

Bernacchi, C.J., Portis, A.R., Nakano, H., von Caemmerer, S. and Long, S.P. (2002) Temperature response of mesophyll conductance. Implications for the determination of Rubisco enzyme kinetics and for limitations to photosynthesis in vivo. *Plant Physiol.* **130**, 1992–1998.

Bernacchi, C.J., Pimentel, C. and Long, S.P. (2003) In vivo temperature response functions of parameters required to model RuBP-limited photosynthesis. *Plant, Cell Environ.* **26**, 1419–1430.

Bernacchi, C.J., Rosenthal, D.M., Pimentel, C., Long, S.P. and Farquhar, G.D. (2009) Modeling the temperature dependence of C3 photosynthesis. In *Photosynthesis In Silico* (Laisk, A., Nedbal, L. and Govindjeeeds). Dordrecht: Springer, Netherlands, pp. 231–246.

Bonan, G.B. (2008) Forests and climate change: forcings, feedbacks, and the climate benefits of forests. *Science*, **320**, 1444–1449.

Bonan, G.B., Lawrence, P.J., Oleson, K.W., Levis, S., Jung, M., Reichstein, M., Lawrence, D.M. and Swenson, S.C. (2011) Improving canopy processes in the Community Land Model version 4 (CLM4) using global flux fields empirically inferred from FLUXNET data. *J. Geophys. Res.* **116**(G2).

Booth, B.B.B., Jones, C.D., Collins, M., Totterdell, I.J., Cox, P.M., Sitch, S., Huntingford, C., Betts, R.A., Harris, G.R. and Lloyd, J. (2012) High sensitivity of future global warming to land carbon cycle processes. *Environ. Res. Lett.* **7**, 024002.

Boucher, O., Jones, A. and Betts, R.A. (2009) Climate response to the physiological impact of carbon dioxide on plants in the Met Office Unified Model HadCM3. *Clim. Dyn.* **32**, 237–249.

von Caemmerer, S. (2000) *Biochemical Models of Leaf Photosynthesis*. Collingwood, Australia: CSIRO Publishing.

von Caemmerer, S. and Evans, J.R. (2015) Temperature responses of mesophyll conductance differ greatly between species. *Plant Cell Environ.* **38**, 629–637.

Cai, T., Flanagan, L.B., Jassal, R.S. and Black, T.A. (2008) Modelling environmental controls on ecosystem photosynthesis and the carbon isotope composition of ecosystem-respired CO_2 in a coastal Douglas-fir forest. *Plant Cell Environ.* **31**, 435–453.

Cano, F.J., Sánchez-Gómez, D., Gascó, A., Rodríguez-Calcerrada, J., Gil, L., Warren, C.R. and Aranda, I. (2011) Light acclimation at the end of the growing season in two broadleaved oak species. *Photosynthetica*, **49**, 581–592.

Cano, F.J., Sharwood, R.E., Cousins, A.B. and Ghannoum, O. (2019) The role of leaf width and conductances to CO_2 in determining water use efficiency in C4 grasses. *New Phytol.* **223**, 1280–1295.

Carriquí, M., Douthe, C., Molins, A. and Flexas, J. (2019) Leaf anatomy does not explain apparent short-term responses of mesophyll conductance to light and CO_2 in tobacco. *Physiol. Plant.* **165**, 604–618.

De Kauwe, M.G., Medlyn, B.E., Zaehle, S. *et al.* (2013) Forest water use and water use efficiency at elevated CO_2: a model-data intercomparison at two contrasting temperate forest FACE sites. *Glob. Change Biol.* **19**, 1759–1779.

Delfine, S., Alvino, A., Villani, M.C. and Loreto, F. (1999) Restrictions to carbon dioxide conductance and photosynthesis in spinach leaves recovering from salt stress. *Plant Physiol.* **119**, 1101–1106.

Dewar, R., Mauranen, A., Mäkelä, Annikki, Hölttä, Teemu, Medlyn, B. and Vesala, T. (2017) New insights into the covariation of stomatal, mesophyll and hydraulic conductances from optimization models incorporating non-stomatal limitations to photosynthesis. *New Phytol.* **217**, 571–585.

Dillaway, D.N. and Kruger, E.L. (2010) Thermal acclimation of photosynthesis: a comparison of boreal and temperate tree species along a latitudinal transect. *Plant Cell Environ.* **33**, 888–899.

Douthe, C., Dreyer, E., Brendel, O. and Warren, C.R. (2012) Is mesophyll conductance to CO_2 in leaves of three Eucalyptus species sensitive to short-term changes of irradiance under ambient as well as low O_2? *Funct. Plant Biol.* **39**, 435–448.

Duursma, R.A. (2015) Plantecophys-an R package for analysing and modelling leaf gas exchange data. *PLoS ONE*, **10**, e0143346.

Egea, G., Verhoef, A. and Vidale, P.L. (2011) Towards an improved and more flexible representation of water stress in coupled photosynthesis-stomatal conductance models. *Agric. For. Meteorol.* **151**, 1370–1384.

Ethier, G.J. and Livingston, N.J. (2004) On the need to incorporate sensitivity to CO_2 transfer conductance into the Farquhar-von Caemmerer-Berry leaf photosynthesis model. *Plant Cell Environ.* **27**, 137–153.

Evans, J.R. and Von Caemmerer, S. (1996) Carbon dioxide diffusion inside leaves. *Plant Physiol.* **110**, 339.

Evans, J.R., Sharkey, T.D., Berry, J.A. and Farquhar, G.D. (1986) Carbon isotope discrimination measured concurrently with gas exchange to investigate CO_2 diffusion in leaves of higher plants. *Funct. Plant Biol.* **13**, 281–292.

Evans, J.R., Caemmerer, S.V., Setchell, B.A. and Hudson, G.S. (1994) The relationship between CO_2 transfer conductance and leaf anatomy in transgenic tobacco with a reduced content of Rubisco. *Funct. Plant Biol.* **21**, 475–495.

Evans, J.R., Kaldenhoff, R., Genty, B. and Terashima, I. (2009) Resistances along the CO_2 diffusion pathway inside leaves. *J. Exp. Bot.* **60**, 2235–2248.

Farquhar, G.D. and Sharkey, T.D. (1982) Stomatal conductance and photosynthesis. *Annu. Rev. Plant Physiol.* **33**, 317–345.

Farquhar, G.D., von Caemmerer, S.V. and Berry, J.A. (1980) A biochemical model of photosynthetic CO_2 assimilation in leaves of C3 species. *Planta*, **149**, 78–90.

Farquhar, G.D., O'leary, M.H. and Berry, J.A. (1982) On the relationship between carbon isotope discrimination and the intercellular carbon dioxide concentration in leaves. *Funct. Plant Biol.* **9**, 121–137.

Flexas, J., Díaz-Espejo, A., Galmés, J., Kaldenhoff, R., Medrano, H. and Ribas-Carbo, M. (2007) Rapid variations of mesophyll conductance in response to changes in CO_2 concentration around leaves. *Plant Cell Environ.* **30**, 1284–1298.

Flexas, J., Ribas-Carbo, M., Díaz-Espejo, A., Galmés, J. and Medrano, H. (2008) Mesophyll conductance to CO_2: current knowledge and future prospects. *Plant Cell Environ.* **31**, 602–621.

Flexas, J., Barbour, M.M., Brendel, O. *et al.* (2012) Mesophyll diffusion conductance to CO_2: an unappreciated central player in photosynthesis. *Plant Sci.* **193**, 70–84.

Flexas, J., Niinemets, Ü., Gallé, A. *et al.* (2013a) Diffusional conductances to CO_2 as a target for increasing photosynthesis and photosynthetic water-use efficiency. *Photosynth. Res.* **117**, 45–59.

Flexas, J., Scoffoni, C., Gago, J. and Sack, L. (2013b) Leaf mesophyll conductance and leaf hydraulic conductance: an introduction to their measurement and coordination. *J. Exp. Bot.* **64**, 3965–3981.

Flexas, J., Díaz-Espejo, A., Conesa, M.A. *et al.* (2016) Mesophyll conductance to CO_2 and Rubisco as targets for improving intrinsic water use efficiency in C3 plants. *Plant Cell Environ.* **39**, 965–982.

Flexas, J., Cano, F.J., Carriquí, M., Coopman, R.E., Mizokami, Y., Tholen, D. and Xiong, D. (2018) CO_2 diffusion inside photosynthetic organs. In *The Leaf: A Platform for Performing Photosynthesis* (Adams, W. W. Illand Terashima, I., eds). Cham: Springer International Publishing, pp. 163–208.

Forkel, M., Carvalhais, N., Rödenbeck, C., Keeling, R., Heimann, M., Thonicke, K., Zaehle, S. and Reichstein, M. (2016) Enhanced seasonal CO_2 exchange caused by amplified plant productivity in northern ecosystems. *Science*, **351**, 696–699.

Frank, D.C., Poulter, B., Saurer, M. *et al.* (2015) Water-use efficiency and transpiration across European forests during the Anthropocene. *Nat. Clim. Chang.* **5**, 579–583.

Franks, P.J., Adams, M.A., Amthor, J.S. *et al.* (2013) Sensitivity of plants to changing atmospheric CO_2 concentration: from the geological past to the next century. *New Phytol.* **197**, 1077–1094.

Friend, A.D. and Kiang, N.Y. (2005) Land surface model development for the GISS GCM: effects of improved canopy physiology on simulated climate. *J. Clim.* **18**, 2883–2902.

Gago, J., Carriquí, M., Nadal, M., Clemente-Moreno, M.J., Coopman, R.E., Fernie, A.R. and Flexas, J. (2019) Photosynthesis optimized across land plant phylogeny. *Trends Plant Sci.* **24**, 947–958.

Galmés, J., Medrano, H. and Flexas, J. (2007) Photosynthetic limitations in response to water stress and recovery in Mediterranean plants with different growth forms. *New Phytol.* **175**, 81–93.

Galmés, J., Hermida-Carrera, C., Laanisto, L. and Niinemets, Ü. (2016) A compendium of temperature responses of Rubisco kinetic traits: variability among and within photosynthetic groups and impacts on photosynthesis modeling. *J. Exp. Bot.* **67**, 5067–5091.

Galmés, J., Capó-Bauçà, S., Niinemets, Ü. and Iñiguez, C. (2019) Potential improvement of photosynthetic CO_2 assimilation in crops by exploiting the natural variation in the temperature response of Rubisco catalytic traits. *Curr. Opin. Plant Biol.* **49**, 60–67.

Gedney, N., Cox, P.M., Betts, R.A., Boucher, O., Huntingford, C. and Stott, P.A. (2006) Detection of a direct carbon dioxide effect in continental river runoff records. *Nature*, **439**, 835–838.

Grassi, G. and Magnani, F. (2005) Stomatal, mesophyll conductance and biochemical limitations to photosynthesis as affected by drought and leaf ontogeny in ash and oak trees. *Plant Cell Environ.* **28**, 834–849.

Gu, L. and Sun, Y. (2014) Artefactual responses of mesophyll conductance to CO_2 and irradiance estimated with the variable J and online isotope discrimination methods. *Plant Cell Environ.* **37**, 1231–1249.

Gu, L., Pallardy, S.G., Tu, K., Law, B.E. and Wullschleger, S.D. (2010) Reliable estimation of biochemical parameters from C3 leaf photosynthesis-intercellular carbon dioxide response curves. *Plant Cell Environ.* **33**, 1852–1874.

Hall, A.E. (1971) A model of leaf photosynthesis and respiration. *Carnegie Inst. Wash. Year Book*, **70**, 530–540.

Han, Q., Iio, A., Naramoto, M. and Kakubari, Y. (2010) Response of internal conductance to soil drought in sun and shade leaves of adult *Fagus crenata*. *Acta Silv. Lign. Hung.* **6**, 123–133.

Hanba, Y.T., Miyazawa, S.-I., Kogami, H. and Terashima, I. (2001) Effects of leaf age on internal CO_2 transfer conductance and photosynthesis in tree species having different types of shoot phenology. *Funct. Plant Biol.* **28**, 1075–1084.

Hanba, Y.T., Kogami, H. and Terashima, I. (2002) The effect of growth irradiance on leaf anatomy and photosynthesis in *Acer* species differing in light demand. *Plant Cell Environ.* **25**, 1021–1030.

Harley, P.C., Loreto, F., Di Marco, G. and Sharkey, T.D. (1992) Theoretical considerations when estimating the mesophyll conductance to CO_2 flux by analysis of the response of photosynthesis to CO_2. *Plant Physiol.* **98**, 1429–1436.

Hassiotou, F., Ludwig, M., Renton, M., Veneklaas, E.J. and Evans, J.R. (2009) Influence of leaf dry mass per area, CO_2, and irradiance on mesophyll conductance in sclerophylls. *J. Exp. Bot.* **60**, 2303–2314.

Jin, S.H., Huang, J.Q., Li, X.Q., Zheng, B.S., Wu, J.S., Wang, Z.J., Liu, G.H. and Chen, M. (2011) Effects of potassium supply on limitations of photosynthesis by mesophyll diffusion conductance in *Carya cathayensis*. *Tree Physiol.* **31**, 1142–1151.

Kattge, J. and Knorr, W. (2007) Temperature acclimation in a biochemical model of photosynthesis: a reanalysis of data from 36 species. *Plant Cell Environ.* **30**, 1176–1190.

Keeling, R.F., Graven, H.D., Welp, L.R., Resplandy, L., Bi, J., Piper, S.C., Sun, Y., Bollenbacher, A. and Meijer, H.A.J. (2017) Atmospheric evidence for a global secular increase in carbon isotopic discrimination of land photosynthesis. *Proc. Natl Acad. Sci. USA*, **114**, 10361–10366.

Keenan, T., Sabaté, S. and Gracia, C. (2010) Soil water stress and coupled photosynthesis-conductance models: bridging the gap between conflicting reports on the relative roles of stomatal, mesophyll conductance and biochemical limitations to photosynthesis. *Agric. For. Meteorol.* **150**, 443–453.

Kitao, M., Yazaki, K., Kitaoka, S., Fukatsu, E., Tobita, H., Komatsu, M., Maruyama, Y. and Koike, T. (2015) Mesophyll conductance in leaves of Japanese white birch (*Betula platyphylla* var. *japonica*) seedlings grown under elevated CO_2 concentration and low N availability. *Physiol. Plant.* **155**, 435–445.

Knauer, J., Zaehle, S., Reichstein, M., Medlyn, B.E., Forkel, M., Hagemann, S. and Werner, C. (2017) The response of ecosystem water-use efficiency to rising atmospheric CO_2 concentrations: sensitivity and large-scale biogeochemical implications. *New Phytol.* **213**, 1654–1666.

Knauer, J., Zaehle, S., De Kauwe, M.G., Bahar, N.H.A., Evans, J.R., Medlyn, B.E., Reichstein, M. and Werner, C. (2019) Effects of mesophyll conductance on vegetation responses to elevated CO_2 concentrations in a land surface model. *Glob. Change Biol.* **25**, 1820–1838.

Kolbe, A.R. and Cousins, A.B. (2018) Mesophyll conductance in *Zea mays* responds transiently to CO_2 availability: implications for transpiration efficiency in C4 crops. *New Phytol.* **217**, 1463–1474.

Kumarathunge, D.P., Medlyn, B.E., Drake, J.E. *et al.* (2018) ACi-TGlob_V1.0: a global dataset of photosynthetic CO_2 response curves of terrestrial plants. https://doi.org/10.6084/m9.figshare.7283567.v1.

Kumarathunge, D.P., Medlyn, B.E., Drake, J.E. *et al.* (2019) Acclimation and adaptation components of the temperature dependence of plant photosynthesis at the global scale. *New Phytol.* **222**, 768–784.

Lauteri, M., Scartazza, A., Guido, M.C. and Brugnoli, E. (1997) Genetic variation in photosynthetic capacity, carbon isotope discrimination and mesophyll conductance in provenances of *Castanea sativa* adapted to different environments. *Funct. Ecol.* **11**, 675–683.

Lemordant, L., Gentine, P., Swann, A.S., Cook, B.I. and Scheff, J. (2018) Critical impact of vegetation physiology on the continental hydrologic cycle in response to increasing CO_2. *Proc. Natl Acad. Sci. USA*, **115**, 4093–4098.

Leuning, R. (1995) A critical appraisal of a combined stomatal-photosynthesis model for C3 plants. *Plant Cell Environ.* **18**, 339–355.

Limousin, J.-M., Misson, L., Lavoir, A.-V., Martin, N.K. and Rambal, S. (2010) Do photosynthetic limitations of evergreen *Quercus ilex* leaves change with long-term increased drought severity? *Plant Cell Environ.* **33**, 863–875.

Long, S.P. and Bernacchi, C.J. (2003) Gas exchange measurements, what can they tell us about the underlying limitations to photosynthesis? Procedures and sources of error. *J. Exp. Bot.* **54**, 2393–2401.

Loucos, K.E., Simonin, K.A. and Barbour, M.M. (2017) Leaf hydraulic conductance and mesophyll conductance are not closely related within a single species. *Plant Cell Environ.* **40**, 203–215.

McNaughton, K.G. and Jarvis, P.G. (1991) Effects of spatial scale on stomatal control of transpiration. *Agric. For. Meteorol.* **54**, 279–302.

Medlyn, B.E., Duursma, R.A., Eamus, D., Ellsworth, D.S., Prentice, I.C., Barton, C.V.M., Crous, K.Y., Angelis, P.D., Freeman, M. and Wingate, L. (2011) Reconciling the optimal and empirical approaches to modelling stomatal conductance. *Glob. Change Biol.* **17**, 2134–2144.

Mizokami, Y., Noguchi, K., Kojima, M., Sakakibara, H. and Terashima, I. (2019a) Effects of instantaneous and growth CO_2 levels and abscisic acid on stomatal and mesophyll conductances. *Plant Cell Environ.* **42**, 1257–1269.

Mizokami, Y., Sugiura, D., Watanabe, C.K.A., Betsuyaku, E., Inada, N. and Terashima, I. (2019b) Elevated CO_2-induced changes in mesophyll conductance and anatomical traits in wild type and carbohydrate-metabolism mutants of Arabidopsis. *J. Exp. Bot.* **70**, 4807–4818.

Montpied, P., Granier, A. and Dreyer, E. (2009) Seasonal time-course of gradients of photosynthetic capacity and mesophyll conductance to CO_2 across a beech (*Fagus sylvatica* L.) canopy. *J. Exp. Bot.* **60**, 2407–2418.

Moualeu-Ngangue, D.P., Chen, T.-W. and Stützel, H. (2017) A new method to estimate photosynthetic parameters through net assimilation rate-intercellular space CO_2 concentration (A–C_i) curve and chlorophyll fluorescence measurements. *New Phytol.* **213**, 1543–1554.

Nadal, M. and Flexas, J. (2018) Mesophyll conductance to CO_2 diffusion: Effects of drought and opportunities for improvement. In *Water Scarcity and Sustainable Agriculture in Semiarid Environment* (García Tejero, I.F. and Durán Zuazo, V.H., eds). London, UK: Academic Press, pp. 403–438.

Nadal, M., Flexas, J. and Gulías, J. (2018) Possible link between photosynthesis and leaf modulus of elasticity among vascular plants: a new player in leaf traits relationships? *Ecol. Lett.* **21**, 1372–1379.

Nakano, H., Muramatsu, S., Makino, A. and Mae, T. (2000) Relationship between the suppression of photosynthesis and starch accumulation in the pod-removed bean. *Funct. Plant Biol.* **27**, 167–173.

Niinemets, Ü. and Reichstein, M. (2003) Controls on the emission of plant volatiles through stomata: a sensitivity analysis. *J. Geophys. Res.* **108** (D7). https://doi.org/10.1029/2002JD002626.

Niinemets, Ü., Cescatti, A., Rodeghiero, M. and Tosens, T. (2006) Complex adjustments of photosynthetic potentials and internal diffusion conductance to current and previous light availabilities and leaf age in Mediterranean evergreen species *Quercus ilex*. *Plant Cell Environ.* **29**, 1159–1178.

Niinemets, Ü., Díaz-Espejo, A., Flexas, J., Galmés, J. and Warren, C.R. (2009) Role of mesophyll diffusion conductance in constraining potential photosynthetic productivity in the field. *J. Exp. Bot.* **60**, 2249–2270.

Niinemets, Ü., Flexas, J. and Peñuelas, J. (2011) Evergreens favored by higher responsiveness to increased CO_2. *Trends Ecol. Evol.* **26**, 136–142.

Ohsumi, A., Hamasaki, A., Nakagawa, H., Yoshida, H., Shiraiwa, T. and Horie, T. (2007) A model explaining genotypic and ontogenetic variation of leaf photosynthetic rate in rice (*Oryza sativa*) based on leaf nitrogen content and stomatal conductance. *Ann. Bot.* **99**, 265–273.

Onoda, Y., Wright, I.J., Evans, J.R., Hikosaka, K., Kitajima, K., Niinemets, Ü., Poorter, H., Tosens, T. and Westoby, M. (2017) Physiological and structural tradeoffs underlying the leaf economics spectrum. *New Phytol.* **214**, 1447–1463.

Osborn, H.L., Alonso-Cantabrana, H., Sharwood, R.E., Covshoff, S., Evans, J.R., Furbank, R.T. and von Caemmerer, S. (2017) Effects of reduced carbonic anhydrase activity on CO_2 assimilation rates in *Setaria viridis*: a transgenic analysis. *J. Exp. Bot.* **68**, 299–310.

Ouyang, W., Struik, P.C., Yin, X. and Yang, J. (2017) Stomatal conductance, mesophyll conductance, and transpiration efficiency in relation to leaf anatomy in rice and wheat genotypes under drought. *J. Exp. Bot.* **68**, 5191–5205.

Peguero-Pina, J.J., Sisó, S., Flexas, J., Galmés, J., García-Nogales, A., Niinemets, Ü., Sancho-Knapik, D., Saz, M.Á. and Gil-Pelegrín, E. (2017) Cell-level anatomical characteristics explain high mesophyll conductance and photosynthetic capacity in sclerophyllous Mediterranean oaks. *New Phytol.* **214**, 585–596.

Pengelly, J.J.L., Förster, B., von Caemmerer, S., Badger, M.R., Price, G.D. and Whitney, S.M. (2014) Transplastomic integration of a cyanobacterial bicarbonate transporter into tobacco chloroplasts. *J. Exp. Bot.* **65**, 3071–3080.

Perez-Martin, A., Flexas, J., Ribas-Carbó, M., Bota, J., Tomás, M., Infante, J.M. and Diaz-Espejo, A. (2009) Interactive effects of soil water deficit and air vapour pressure deficit on mesophyll conductance to CO_2 in *Vitis vinifera* and *Olea europaea*. *J. Exp. Bot.* **60**, 2391–2405.

Perez-Martin, A., Michelazzo, C., Torres-Ruiz, J.M., Flexas, J., Fernández, J.E., Sebastiani, L. and Diaz-Espejo, A. (2014) Regulation of photosynthesis and stomatal and mesophyll conductance under water stress and recovery in olive trees: correlation with gene expression of carbonic anhydrase and aquaporins. *J. Exp. Bot.* **65**, 3143–3156.

Peters, W., van der Velde, I.R., van Schaik, E. *et al.* (2018) Increased water-use efficiency and reduced CO_2 uptake by plants during droughts at a continental scale. *Nat. Geosci.* **11**, 744.

Pons, T.L., Flexas, J., Von Caemmerer, S., Evans, J.R., Genty, B., Ribas-Carbó, M. and Brugnoli, E. (2009) Estimating mesophyll conductance to CO_2: methodology, potential errors, and recommendations. *J. Exp. Bot.* **60**, 2217–2234.

Rogers, A., Medlyn, B.E., Dukes, J.S. *et al.* (2017) A roadmap for improving the representation of photosynthesis in Earth system models. *New Phytol.* **213**, 22–42.

Sawada, S., Kuninaka, M., Watanabe, K., Sato, A., Kawamura, H., Komine, K., Sakamoto, T. and Kasai, M. (2001) The mechanism to suppress photosynthesis through end-product inhibition in single-rooted soybean leaves during acclimation to CO_2 enrichment. *Plant Cell Physiol.* **42**, 1093–1102.

Scholze, M., Ciais, P. and Heimann, M. (2008) Modeling terrestrial ^{13}C cycling: climate, land use and fire. *Global Biogeochem. Cycles*, **22**, GB1009. https://doi.org/10.1029/2006GB002899

Seibt, U., Rajabi, A., Griffiths, H. and Berry, J.A. (2008) Carbon isotopes and water use efficiency: sense and sensitivity. *Oecologia*, **155**, 441–454.

Sellers, P.J., Bounoua, L., Collatz, G.J. *et al.* (1996) Comparison of radiative and physiological effects of doubled atmospheric CO_2 on climate. *Science*, **271**, 1402–1405.

Shrestha, A., Song, X. and Barbour, M.M. (2019) The temperature response of mesophyll conductance, and its component conductances, varies between species and genotypes. *Photosynth. Res.* **141**, 65–82.

Silim, S.N., Ryan, N. and Kubien, D.S. (2010) Temperature responses of photosynthesis and respiration in *Populus balsamifera* L.: acclimation versus adaptation. *Photosynth. Res.* **104**, 19–30.

Singsaas, E.L., Ort, D.R. and Delucia, E.H. (2003) Elevated CO_2 effects on mesophyll conductance and its consequences for interpreting photosynthetic physiology. *Plant Cell Environ.* **27**, 41–50.

Sjögersten, S., van der Wal, R. and Woodin, S.J. (2006) Small-scale hydrological variation determines landscape CO_2 fluxes in the high Arctic. *Biogeochemistry*, **80**, 205–216.

Smith, N.G., Malyshev, S.L., Shevliakova, E., Kattge, J. and Dukes, J.S. (2016) Foliar temperature acclimation reduces simulated carbon sensitivity to climate. *Nat. Clim. Chang.* **6**, 407–411.

Smith, N.G., Lombardozzi, D., Tawfik, A., Bonan, G. and Dukes, J.S. (2017) Biophysical consequences of photosynthetic temperature acclimation for climate. *J. Adv. Model. Earth Syst.* **9**, 536–547.

Suits, N.S., Denning, A.S., Berry, J.A., Still, C.J., Kaduk, J., Miller, J.B. and Baker, I.T. (2005) Simulation of carbon isotope discrimination of the terrestrial biosphere. *Global Biogeochem. Cycles*, **19**. https://doi.org/10.1029/2003GB002141

Sun, Y., Gu, L., Dickinson, R.E., Norby, R.J., Pallardy, S.G. and Hoffman, F.M. (2014a) Impact of mesophyll diffusion on estimated global land CO_2 fertilization. *Proc. Natl Acad. Sci. USA*, **111**, 15774–15779.

Sun, Y., Gu, L., Dickinson, R.E. *et al.* (2014b) Asymmetrical effects of mesophyll conductance on fundamental photosynthetic parameters and their

relationships estimated from leaf gas exchange measurements. *Plant Cell Environ.* **37**, 978–994.

Tazoe, Y., Von Caemmerer, S., Badger, M.R. and Evans, J.R. (2009) Light and CO_2 do not affect the mesophyll conductance to CO_2 diffusion in wheat leaves. *J. Exp. Bot.* **60**, 2291–2301.

Terashima, I., Hanba, Y.T., Tazoe, Y., Vyas, P. and Yano, S. (2006) Irradiance and phenotype: comparative eco-development of sun and shade leaves in relation to photosynthetic CO_2 diffusion. *J. Exp. Bot.* **57**, 343–354.

Terashima, I., Hanba, Y.T., Tholen, D. and Niinemets, Ü. (2011) Leaf functional anatomy in relation to photosynthesis. *Plant Physiol.* **155**, 108–116.

Théroux-Rancourt, G. and Gilbert, M.E. (2017) The light response of mesophyll conductance is controlled by structure across leaf profiles. *Plant Cell Environ.* **40**, 726–740.

Tholen, D. and Zhu, X.-G. (2011) The mechanistic basis of internal conductance: a theoretical analysis of mesophyll cell photosynthesis and CO_2 diffusion. *Plant Physiol.* **156**, 90–105.

Tholen, D., Ethier, G., Genty, B., Pepin, S. and Zhu, X.-G. (2012) Variable mesophyll conductance revisited: theoretical background and experimental implications. *Plant Cell Environ.* **35**, 2087–2103.

Tomás, M., Flexas, J., Copolovici, L., Galmés, J., Hallik, L., Medrano, H., Ribas-Carbó, M., Tosens, T., Vislap, V. and Niinemets, Ü. (2013) Importance of leaf anatomy in determining mesophyll diffusion conductance to CO_2 across species: quantitative limitations and scaling up by models. *J. Exp. Bot.* **64**, 2269–2281.

Turetsky, M.R., Bond-Lamberty, B., Euskirchen, E., Talbot, J., Frolking, S., McGuire, A.D. and Tuittila, E.-S. (2012) The resilience and functional role of moss in boreal and arctic ecosystems. *New Phytol.* **196**, 49–67.

Ubierna, N. and Farquhar, G.D. (2014) Advances in measurements and models of photosynthetic carbon isotope discrimination in C3 plants. *Plant Cell Environ.* **37**, 1494–1498.

Ubierna, N., Gandin, A., Boyd, R.A. and Cousins, A.B. (2017) Temperature response of mesophyll conductance in three C_4 species calculated with two methods: ^{18}O discrimination and *in vitro* V_{pmax}. *New Phytol.* **214**, 66–80.

Ubierna, N., Gandin, A. and Cousins, A.B. (2018) The response of mesophyll conductance to short-term variation in CO_2 in the C4 plants *Setaria viridis* and *Zea mays*. *J. Exp. Bot.* **69**, 1159–1170.

Varone, L., Ribas-Carbó, M., Cardona, C., Gallé, A., Medrano, H., Gratani, L. and Flexas, J. (2012) Stomatal and non-stomatal limitations to photosynthesis in seedlings and saplings of Mediterranean species pre-conditioned and aged in nurseries: Different response to water stress. *Environ. Exp. Bot.* **75**, 235–247.

Verhoef, A. and Egea, G. (2014) Modeling plant transpiration under limited soil water: comparison of different plant and soil hydraulic parameterizations and preliminary implications for their use in land surface models. *Agric. For. Meteorol.* **191**, 22–32.

Veromann-Jürgenson, L.-L., Tosens, T., Laanisto, L. and Niinemets, Ü. (2017) Extremely thick cell walls and low mesophyll conductance: welcome to the world of ancient living! *J. Exp. Bot.* **68**, 1639–1653.

Vico, G. and Porporato, A. (2008) Modelling C3 and C4 photosynthesis under water-stressed conditions. *Plant Soil*, **313**, 187–203.

Vrábl, D., Vašková, M., Hronková, M., Flexas, J. and Šantrůček, J. (2009) Mesophyll conductance to CO_2 transport estimated by two independent methods: effect of variable CO_2 concentration and abscisic acid. *J. Exp. Bot.* **60**, 2315–2323.

Walker, B., Ariza, L.S., Kaines, S., Badger, M.R. and Cousins, A.B. (2013) Temperature response of *in vivo* Rubisco kinetics and mesophyll conductance in *Arabidopsis thaliana*: comparisons to *Nicotiana tabacum*. *Plant Cell Environ.* **36**, 2108–2119.

Wang, X., Du, T., Huang, J., Peng, S. and Xiong, D. (2018a) Leaf hydraulic vulnerability triggers the decline in stomatal and mesophyll conductance during drought in rice. *J. Exp. Bot.* **69**, 4033–4045.

Wang, X., Wang, W., Huang, J., Peng, S. and Xiong, D. (2018b) Diffusional conductance to CO_2 is the key limitation to photosynthesis in salt-stressed leaves of rice (*Oryza sativa*). *Physiol. Plant.* **163**, 45–58.

Warren, C.R. (2006) Why does photosynthesis decrease with needle age in *Pinus pinaster*? *Trees*, **20**, 157–164.

Warren, C.R. (2008a) Does growth temperature affect the temperature responses of photosynthesis and internal conductance to CO_2? A test with *Eucalyptus regnans*. *Tree Physiol.* **28**, 11–19.

Warren, C.R. (2008b) Stand aside stomata, another actor deserves centre stage: the forgotten role of the internal conductance to CO_2 transfer. *J. Exp. Bot.* **59**, 1475–1487.

Warren, C.R., Löw, M., Matyssek, R. and Tausz, M. (2007) Internal conductance to CO_2 transfer of adult *Fagus sylvatica*: Variation between sun and shade leaves and due to free-air ozone fumigation. *Environ. Exp. Bot.* **59**, 130–138.

Wei, Z., Yoshimura, K., Wang, L., Miralles, D.G., Jasechko, S. and Lee, X. (2017) Revisiting the contribution of transpiration to global terrestrial evapotranspiration. *Geophys. Res. Lett.* **44**, 2792–2801.

Wingate, L., Seibt, U., Moncrieff, J.B., Jarvis, P.G. and Lloyd, J.O.N. (2007) Variations in ^{13}C discrimination during CO_2 exchange by *Picea sitchensis* branches in the field. *Plant Cell Environ.* **30**, 600–616.

Xiao, Y. and Zhu, X.-G. (2017) Components of mesophyll resistance and their environmental responses: a theoretical modelling analysis. *Plant Cell Environ.* **40**, 2729–2742.

Xiong, D. and Flexas, J. (2018) Leaf economics spectrum in rice: leaf anatomical, biochemical, and physiological trait trade-offs. *J. Exp. Bot.* **69**, 5599–5609.

Xiong, D., Liu, X., Liu, L., Douthe, C., Li, Y., Peng, S. and Huang, J. (2015) Rapid responses of mesophyll conductance to changes of CO_2 concentration, temperature and irradiance are affected by N supplements in rice. *Plant Cell Environ.* **38**, 2541–2550.

Xiong, D., Flexas, J., Yu, T., Peng, S. and Huang, J. (2017) Leaf anatomy mediates coordination of leaf hydraulic conductance and mesophyll conductance to CO_2 in *Oryza*. *New Phytol.* **213**, 572–583.

Xiong, D., Douthe, C. and Flexas, J. (2018) Differential coordination of stomatal conductance, mesophyll conductance and leaf hydraulic conductance in response to changing light across species. *Plant Cell Environ.* **41**, 436–450.

Xu, Y., Feng, Z., Shang, B., Dai, L., Uddling, J. and Tarvainen, L. (2019) Mesophyll conductance limitation of photosynthesis in poplar under elevated ozone. *Sci. Total Environ.* **657**, 136–145.

Yamori, W., Noguchi, K., Hanba, Y.T. and Terashima, I. (2006) Effects of internal conductance on the temperature dependence of the photosynthetic rate in spinach leaves from contrasting growth temperatures. *Plant Cell Physiol.* **47**, 1069–1080.

Yamori, W., Evans, J.R. and Von Caemmerer, S. (2010) Effects of growth and measurement light intensities on temperature dependence of CO_2 assimilation rate in tobacco leaves. *Plant, Cell Environ.* **33**, 332–343.

Yamori, W., Nagai, T. and Makino, A. (2011) The rate-limiting step for CO_2 assimilation at different temperatures is influenced by the leaf nitrogen content in several C3 crop species. *Plant Cell Environ.* **34**, 764–777.

Yin, X. and Struik, P.C. (2017) Simple generalisation of a mesophyll resistance model for various intracellular arrangements of chloroplasts and mitochondria in C3 leaves. *Photosynth. Res.* **132**, 211–220.

Yin, X., Struik, P.C., Romero, P., Harbinson, J., Evers, J.B., Van Der Putten, P.E.L. and Vos, J. (2009) Using combined measurements of gas exchange and chlorophyll fluorescence to estimate parameters of a biochemical C3 photosynthesis model: a critical appraisal and a new integrated approach applied to leaves in a wheat (*Triticum aestivum*) canopy. *Plant Cell Environ.* **32**, 448–464.

Yin, L., Xu, H., Dong, S., Chu, J., Dai, X. and He, M. (2019) Optimised nitrogen allocation favours improvement in canopy photosynthetic nitrogen-use efficiency: evidence from late-sown winter wheat. *Environ. Exp. Bot.* **159**, 75–86.

Zhang, S.-B. and Yin, L.-X. (2012) Plasticity in photosynthesis and functional leaf traits of *Meconopsis horridula* var. racemosa in response to growth irradiance. *Bot. Stud.* **53**, 335–343.

Zhou, S., Duursma, R.A., Medlyn, B.E., Kelly, J.W.G. and Prentice, I.C. (2013) How should we model plant responses to drought? An analysis of stomatal and non-stomatal responses to water stress. *Agric. For. Meteorol.* **182**, 204–214.

Zhou, S., Medlyn, B., Sabaté, S., Sperlich, D. and Prentice, I.C. (2014) Short-term water stress impacts on stomatal, mesophyll and biochemical limitations to photosynthesis differ consistently among tree species from contrasting climates. *Tree Physiol.* **34**, 1035–1046.

Zhou, H., Akçay, E. and Helliker, B.R. (2019) Estimating C4 photosynthesis parameters by fitting intensive A/C_i curves. *Photosynth. Res.* **141**, 181–194.

